UNIVERSITAT POLITÈCNICA DE VALÈNCIA

DEPARTAMENTO DE BIOTECNOLOGÍA

Promotion of axonal outgrowth and regeneration in cortical neurons by Rho inhibition

TRABAJO FIN DE MÁSTER EN BIOTECNOLOGÍA BIOMÉDICA

ALUMNO/A: Marta Nadal Muñoz

TUTOR/A: Máximo Ibo Galindo Orozco

COTUTOR/A: Pietro Fazzari

Curso Académico: 2019-2020

VALENCIA, 5 junio de 2020

TABLE OF CONTENTS

ABSTRACT

Brain stroke is a pathology characterised by a restriction in the availability of oxygen and nutrients due to poor blood flow. Depending on the cause, an occlusion or the rupture of a vessel, they are classified into ischemic and haemorrhagic, respectively. The core of the stroke is characterised by neuronal loss, while the immediately adjacent area, the penumbra, is represented by damaged alive cells. The physiological regeneration and plasticity of neurons in the penumbra is poor and slow. Therefore, it is important to develop strategies to promote the capability of regeneration and new synapsis establishment of these penumbra neurons. Axon repulsion cues activate Rho pathway avoiding axon outgrowth and, therefore, we propose using an inhibitor of ROCK to improve axonal elongation and regeneration.

In this work we have determined the best concentrations and treatment durations of the inhibitor Fasudil to primary neuronal culture of mouse neurons carrying out three assays. First, we tested different concentrations of Fasudil for 30 minutes to study axon growth cone structure. Second, we administrated the same concentrations for 24 hours and 48 hours to study axonal elongation. And third, we tested same concentrations for 24 hours in an *in vitro* model of axonal injury and regeneration.

We did not see significant results in the first assay by measuring the area and perimeter of the growth cones, however, this could be a consequence of its very dynamic nature. In the second and third assays we saw significant results measuring axonal length with p-values < 0.001 with 50 and 100 µM concentrations. However, 200 µM seemed to be toxic and we stopped using this concentration.

In summary, Fasudil seems to effectively promote axon outgrowth in primary neuronal cultures after 24 and 48 hours and in the injury model after 24 hours with 50 and 100 µM concentrations.

Keywords: Stroke, RhoA, ROCK, Fasudil, axon outgrowth, growth cone.

RESUMEN

El accidente cerebrovascular es una patología caracterizada por la restricción de la disponibilidad de oxígeno y nutrientes debido a un flujo sanguíneo deficiente. Dependiendo de la causa, la oclusión o la rotura de un vaso, se clasifican en isquémico y hemorrágico respectivamente. El núcleo de la lesión se caracteriza por una pérdida de neuronas, mientras que, la zona inmediatamente adyacente, la penumbra, está representada por neuronas vivas dañadas. Por tanto, es importante desarrollar estrategias para promover la capacidad de regeneración y el establecimiento de nuevas sinapsis de las neuronas de la zona de penumbra. Las señales de repulsión axonal activan la vía de Rho evitando el crecimiento axonal y, de esta manera, proponemos el uso de un inhibidor de ROCK para mejorar la elongación y regeneración axonal.

En este trabajo hemos determinado las mejores concentraciones y duraciones del tratamiento del inhibidor Fasudil en cultivos primarios de neuronas de ratón llevando a cabo tres ensayos. Primero, hemos testado diferentes concentraciones de Fasudil durante 30 minutos para estudiar la estructura del cono de crecimiento axonal. En segundo lugar, hemos administrado esas mismas concentraciones durante 24 y 48 horas per a estudiar la elongación axonal. Y, en tercer lugar, hemos probado esas concentraciones durante 24 horas en un modelo *in vitro* de lesión y regeneración axonal.

En el primer ensayo no vimos resultados significativos midiendo el área y perímetro de los conos de crecimiento, no obstante, podría deberse a la naturaleza tan dinámica de dichas estructuras. En el segundo y tercer ensayos obtuvimos resultados significativos midiendo la longitud axonal con p-valores < 0.001 con las concentraciones 50 µM y 100 µM. Sin embargo, la concentración de 200 µM parece resultar tóxica y dejamos de utilizarla.

En resumen, el inhibidor Fasudil parece promover eficazmente el crecimiento axonal en cultivos neuronales primarios tras 24 y 48 horas de tratamiento y tras 24 horas en el modelo de lesión con concentraciones de 50 µM y 100 µM.

Palabras clave: Accidente cerebrovascular, RhoA, ROCK, Fasudil, crecimiento axonal, cono de crecimiento.

RESUM

L'accident cerebrovascular és una patologia caracteritzada per la restricció de la disponibilitat d'oxigen i nutrients degut a un flux sanguini deficient. Depenent de la causa, l'oclusió o la ruptura d'un vas, es classifiquen en isquèmic o hemorràgic. El nucli de la lesió es caracteritza per la pèrdua de neurones, mentre que, la zona immediatament adjacent, la penombra, està representada per neurones vives però danyades. Per tant, és important desenvolupar estratègies per a promoure la capacitat de regeneració i l'establiment de noves sinapsis de les neurones de la zona de penombra. Les senyals de repulsió axonal activen la via de Rho evitant el creixement axonal i, per això, proposem l'ús d'un inhibidor de ROCK per a millorar l'elongació i la regeneració axonal.

En aquest treball hem determinat les millors concentracions i durades de tractament de l'inhibidor Fasudil en cultius primaris de neurones de ratolí duent a terme tres assajos. En primer lloc, hem testat diferents concentracions de Fasudil durant 30 minuts per estudiar l'estructura del con de creixement axonal. Segon, hem administrat les mateixes concentracions durant 24 i 48 hores per a estudiar l'elongació axonal. I, en tercer lloc, hem provat eixes concentracions durant 24 hores en un model *in vitro* de lesió i regeneració axonal.

En el primer assaig no vam veure resultats significatius mesurant l'àrea i el perímetre del cons de creixement, no obstant això, podria ser degut a la naturalesa tan dinàmica d'aquestes estructures. En el segon i tercer obtinguérem resultats significatius mesurant la llargària dels axons amb p-valors < 0.001 amb les concentracions 50 µM i 100 µM. Però la concentració 200 µM pareix resultar tòxica i deixàrem d'utilitzar-la.

En resum, l'inhibidor Fasudil pareix promoure eficaçment el creixement axonal en cultius neuronals primaris després de 24 i 48 hores de tractament i després de 24 hores en el model de lesió amb concentracions de 50 µM i 100 µM.

Paraules clau: Accident cerebrovascular, RhoA, ROCK, Fasudil, creixement axonal, con de creixement.

ABBREVIATIONS

Abbreviation	Term
ACTH	Adrenocorticotropic hormone
CNS	Central nervous system
CRF	Corticotrophin-releasing factor
CSPG	Chondroitin sulfate proteoglycans
D	Post-culture day
E	Embryonic day
ENS	Enteric nervous system
GAP	GTPase activating proteins
GDF	GDI displacement factor
GDI	Guanine nucleotide dissociation inhibitor
GEF	Guanine nucleotide exchange factors
NGR	Nogo receptor
LAR	Leukocyte common antigen–related receptor
LIMK	LIM domain kinase
PBS	Phosphate Buffered Saline
PFA	Paraformaldehyde
PTPσ	Receptor type protein tyrosine phosphatase-sigma
ROCK	Rho associated coiled-coil kinase
RT	Room temperature
SCI	Spinal cord injury

INTRODUCTION

Stroke

Stroke is defined by the World Health Organization as "rapidly developed clinical signs of focal (or global) disturbance of cerebral function, lasting more than 24 hours or leading to death, with no apparent cause other than of vascular origin" (Aho et al., 1980).

Stroke can be classified into ischemic and haemorrhagic (Donnan, Fisher, Macleod, & Davis, 2008). Ischemic stroke represents approximately the 85% of strokes in occidental countries. However, more haemorrhagic strokes are reported in Africa with a ratio of 66:34 ischemic to haemorrhagic (Guzik & Bushnell, 2017; Kalaria, Akinyemi, & Ihara, 2016). Despite of the fact that ischemic stroke is more frequent, haemorrhagic stroke has higher mortality rates. This also means that an ischemic stroke is more likely to lead to psychiatric morbidity.

Pathophysiology

Haemorrhagic stroke occurs as a consequence of an abnormal vascular structure or the rupture of a blood vessel. The most common cause of these ruptures is hypertensive small-vessel disease and about two-thirds of patients had been diagnosed with hypertension before the stroke (Donnan et al., 2008).

On the other hand, ischemic stroke results from the interruption of the blood supply to the brain due to thrombosis, embolism, systemic hypoperfusion, venous thrombosis or, in most cases, to unknown cause, which is diagnosed as cryptogenic. Regardless of the cause, this lack of blood results in a reduction of oxygen and glucose. This anoxia interrupts important processes as cellular metabolism and energy production (Koh & Park, 2017). Loss of intracellular ATP and ionic alteration elicits in death of cells of ischemic core by oncosis, which is characterised by swelling of the organelles, plasma membrane disruption and the consequently cell death. Penumbra zone (**Figure 1**) is characterised by neurons metabolically active which do not have electric activity but hours after stroke, they will start receiving deleterious signals from the dead cells of the ischemic core. Before getting the commitment point, after which apoptosis is inevitable, cells can recover being an interest target to develop therapies (Puig, Brenna, & Magnus, 2018).

Current treatments

Cognitive impairment is a very common consequence after a stroke; however, it depends on factors such as location and volume of the stroke, pre-existing cognitive pathologies

or risk factors like hypertension, atrial fibrillation or diabetes mellitus (Kalaria et al., 2016). For this reason, stroke is considered as a clinical emergency where the decisions taken in the first minutes are very important. An effective, and the only approved, treatment for acute ischemic stroke is the intravenous thrombolysis by the administration of tissue plasminogen activator (IV tPA) (Cheng & Kim, 2015). Another treatment is the administration of aspirin, as it is a cheap, easy to administer compound with low toxic effects. However, only a very few patients are benefited, and it is probably more useful to prevent than to treat. Finally, decompressive surgery is practised to those patients who suffer the combination of malignant middle-cerebral-artery-territory infarction and space-occupying brain oedema (Donnan et al., 2008).

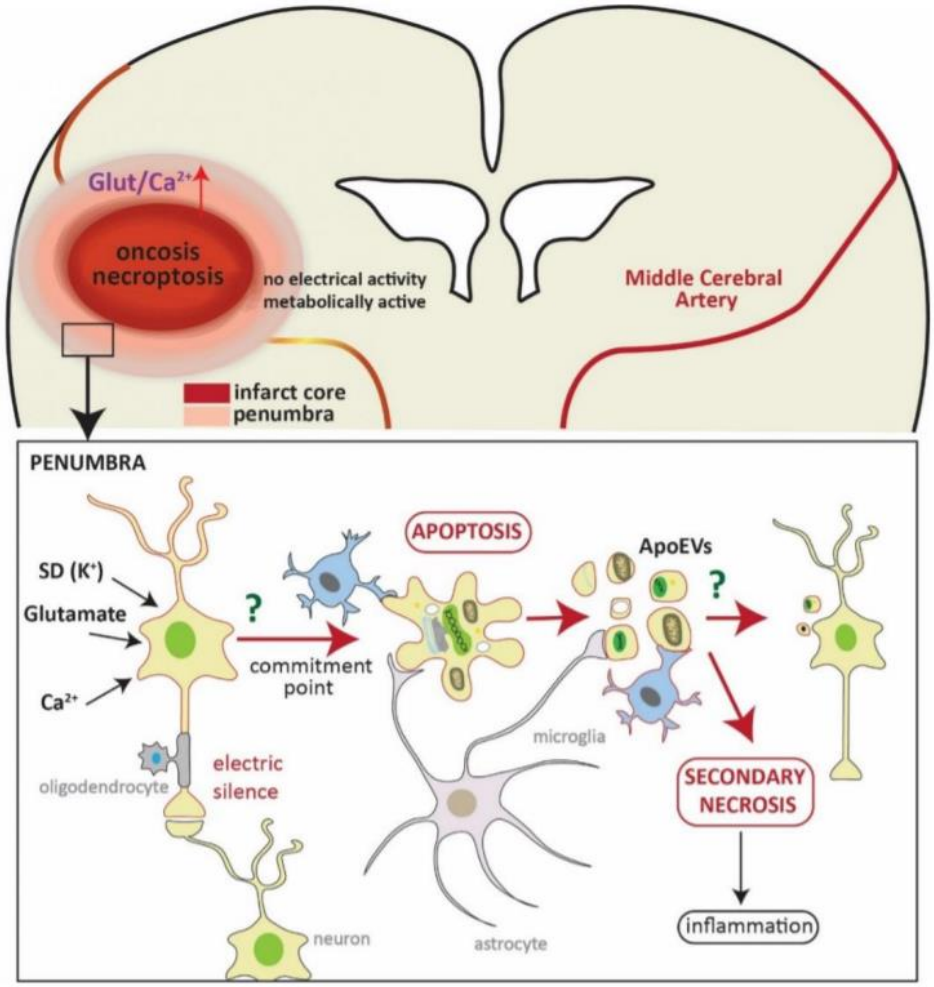

Figure 1: Scheme of neuronal death in penumbra. Up) An occlusion in the middle artery (yellow line) results in oncosis of the ischemic core. Penumbra neurons are metabolically active but do not show electrical activity. Down) They receive deleterious signals from core cells, and they can die by apoptosis or be recovered. If they get to the commitment point, they die by apoptosis being able to trigger secondary necrosis and inflammation. Taken from Puig, Brenna, & Magnus, 2018.

After a stroke, many patients may be dehydrated, so every patient should be monitored for the next 72 hours after stroke to ensure stability of physiological parameters. Those patients who experience severe stroke, complications or comorbidity usually need rehabilitation and palliative care. Patients may also suffer dysphagia, urinary incontinence, communication problems as dysphasia or dysarthria, poor concentration and memory problems or mood disorders (Rodgers, 2013).

Despite the effectiveness of the aforementioned tPA treatment, compounds that can be administered within a few days after ischemic stroke are needed. Late stages in ischemic injury and cognitive impairment are usually consequence of the secondary injury mechanisms as inflammatory reactions, hemorheological abnormalities, vasoconstriction, and endothelial dysfunction. Due to this, it is important to find therapies which decrease these secondary injury mechanisms with a wide therapeutic window (Shibuya, Hirai, Seto, Satoh, & Ohtomo, 2005).

Neurogenesis and neuroplasticity after stroke

After a stroke, it is important to promote neurogenesis from neural stem differentiation and to promote neuroplasticity, which is the capability of the brain to reorganize and create new connections between the undamaged neurons of penumbra zone (Dąbrowski et al., 2019).

Neural stem cells can be damaged after a stroke. A gliosis occurs as a consequence of an abnormal neural stem differentiation, who differentiate into a much greater proportion of astrocytes and lower proportions of neurons, oligodendrocytes and ependymal cells. Enhancing neurogenesis from neural stem cells might be an approach which has been studied by stimulating pathways as Notch, PI3K, Wnt/beta-catenin or Sonic Hedgehog. These pathways promote proliferation, migration and differentiation resulting in neurogenesis and neuroplasticity (Koh & Park, 2017).

Neuronal plasticity is fundamental to guarantee synaptic connections and maintaining neuronal networks, but the glial scar formed after an ischemic stroke avoids the effective regeneration of axons. Epigenetic regulation, as DNA methylation and histone modifications, has an important role in this process. However, the axon regrowth is the most important requirement to promote neuroplasticity after an ischemic stroke. Lots of neurobiological modifications are involved in this regrowth, being the level of myelination and synapse formation examples of it (Dąbrowski et al., 2019). Growth cone guidance molecules are very important in synaptic plasticity through the synthesis of local protein or by the response to specific calcium channel activities (Hou, Jiang, & Smith, 2008). One example is Semaphorin 3A (Sema3A), a secreted guidance cue which induces

the growth cone collapse through the promotion of RhoA mRNA translation and the consequently activation of RhoA pathway (Wu et al., 2005). Nevertheless, Sema3A is not the only axon repulsion cue which activates RhoA, accordingly, inhibiting this pathway could be an interesting approach to develop strategies to promote neuronal plasticity after stroke.

Fasudil

Fasudil is a Rho associated coiled-coil kinase (ROCK) inhibitor whose pathway (Rho/ROCK) plays an important role in axonal growth as it has been described at the previous section. This drug has been used in Japan since 1995 for cerebral vasospasm after aneurysmal subarachnoid haemorrhage (Shibuya et al., 1992) and it has been studied in different diseases included stroke. In 2005 a clinical trial to study the effectivity and safeness of Fasudil in stroke was carried out by Shibuya's group and results were positive (Shibuya et al., 2005).

Rho GTPases and their regulation

Rho is a highly conserved small GTPase family which contains 20 members divided in subfamilies. The Rho subfamily is formed by the three highly homologous isoforms RhoA, RhoB and RhoC. Their signalling research covers all fields of biology as Rho GTPases regulate a lot of cellular processes like cytoskeletal and cell adhesion dynamics, embryogenesis or brain development (Hodge & Ridley, 2016; Narumiya & Thumkeo, 2018). Moreover, they have shown to have a clear implication in different diseases such as cancer (Haga & Ridley, 2016) or mental retardation (Govek et al., 2004).

Small GTPases are typically 20-25 kDa in size and alternate between two forms: the GDP-bound which is usually considered inactive and the GTP-bound which switches on downstream pathways (Cherfils & Zeghouf, 2013). Accordingly, these GTPases incorporate GTP to be activated through guanine nucleotide exchange factors (GEF) while a GTP hydrolysis to GDP catalysed by GTPase activating proteins (GAP) results in the inactivation of Rho GTPases associated with GDP. These ones are in the cytosol forming a complex with guanine nucleotide dissociation inhibitor (RhoGDI). In order to be activated it has to be dissociated from RhoGDI by GDI displacement factor (GDF). Effector proteins bind to activated Rho GTPases to bring about the downstream signalling to target proteins (**Figure 2**) (Kim et al., 2018).

GEFs and GAPs are usually multidomain proteins which stablish protein or lipid interactions with their corresponding domains acting as localization signals or scaffolds for the formation of complexes. These proteins may be regulated, for example, by protein

interactions or second messengers (Bos, Rehmann, & Wittinghofer, 2007). Small GTPases have a high affinity for GDP and GTP, which results in a slow dissociation, however, GEFs and GAPs accelerate the exchange allowing biological processes to occur in minutes or less (Vetter & Wittinghofer, 2001).

Rho GTPases are associated with membranes by an isoprenyl lipid attached to their C-terminal cysteine (Dransart, Olofsson, & Cherfils, 2005). RhoGDI participate in the Rho GTPases regulation solubilizing them in the cytosol and inhibiting the capability of Rho to do the exchange and to hydrolyse GTP. It is also probable that RhoGDI limits the accessibility to GEFs and GAPs. We can find three RhoGDIs in mammals: RhoGDIα which is expressed constitutively, RhoGDIβ expressed in hematopoietic cells (B and T cells particularly) and RhoGDIγ expressed in tissues such as brain or pancreas (Dovas & Couchman, 2005).

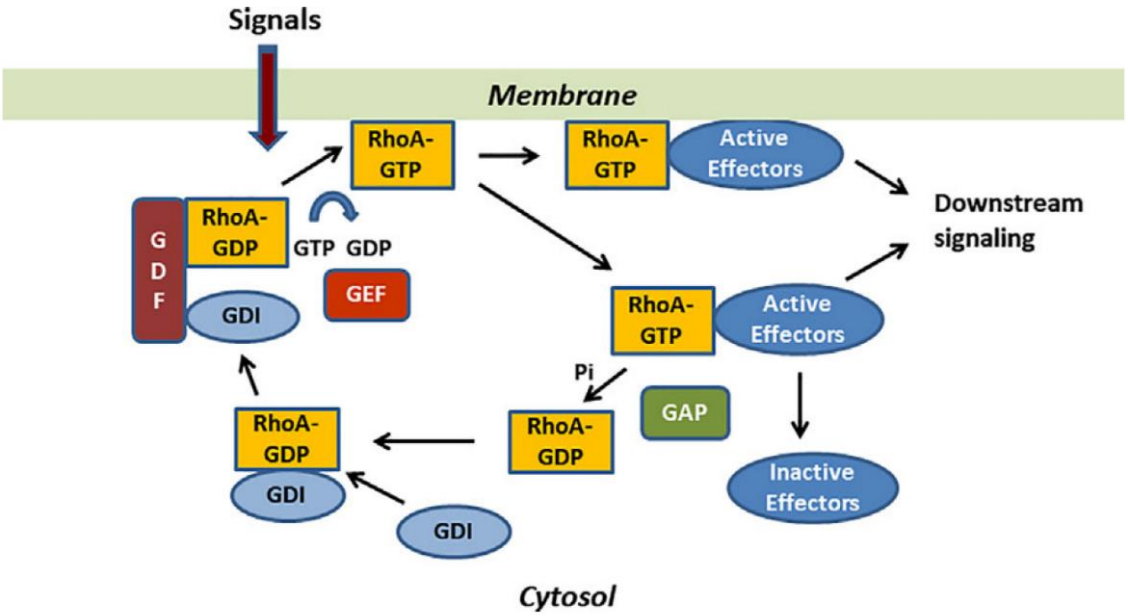

Figure 2: Activation and inactivation of RhoA scheme cycle. The picture shows the alternation of Rho GTPases between GDP and GTP bound as well as all the factors that take part in the pathway: GEF/GAP, GDI, GDF and effector factors. Taken from Kim et al., 2018.

Although a conserved GDF for Rab (another GTPase subfamily) has been found, it is not clear for Rho (Garcia-Mata, Boulter, & Burridge, 2011). Despite this, there are some proteins like ezrin/radixin/moesin (ERM), the neurotrophin receptor p75NTR or IκB kinase γ (IKKγ or NEMO, an essential NF-κB modulator) that have shown to have a GDF activity for Rho (Dransart et al., 2005; Kim et al., 2018).

Despite their implication in many activities and cell processes, Rho GTPases do not have a clear protein domain to, for example, interact with the cytoskeleton. Their functions are

made, therefore, through effector proteins such as ROCK, Rhotekin, Rhophilin, PKN, Citron and mDia (Thumkeo, Watanabe, & Narumiya, 2013).

ROCK

ROCK plays an important role in axon growth inhibiting this process. ROCK is activated by RhoA and belongs to the AGC (PKA, PKG and PKC) family of serine-threonine kinases (J. Liu et al., 2018). There are two isoforms known as ROCK1 and ROCK2 (β and α respectively) with a high homology and similar organs/tissues distribution patterns. However, they are regulated by common and unique mechanisms and while ROCK1 has a significant higher expression in the thymus and blood, ROCK2 is mostly expressed in the brain and the spinal cord (Duffy et al., 2009). Both consist of a catalytic kinase domain at the N-terminal, the central coiled-coil domain which contains the Rho-binding domain (RBD) and the C-terminal pleckstrin homology (PH) domain with an internal cysteine-rich domain (Nakagawa et al., 1996).

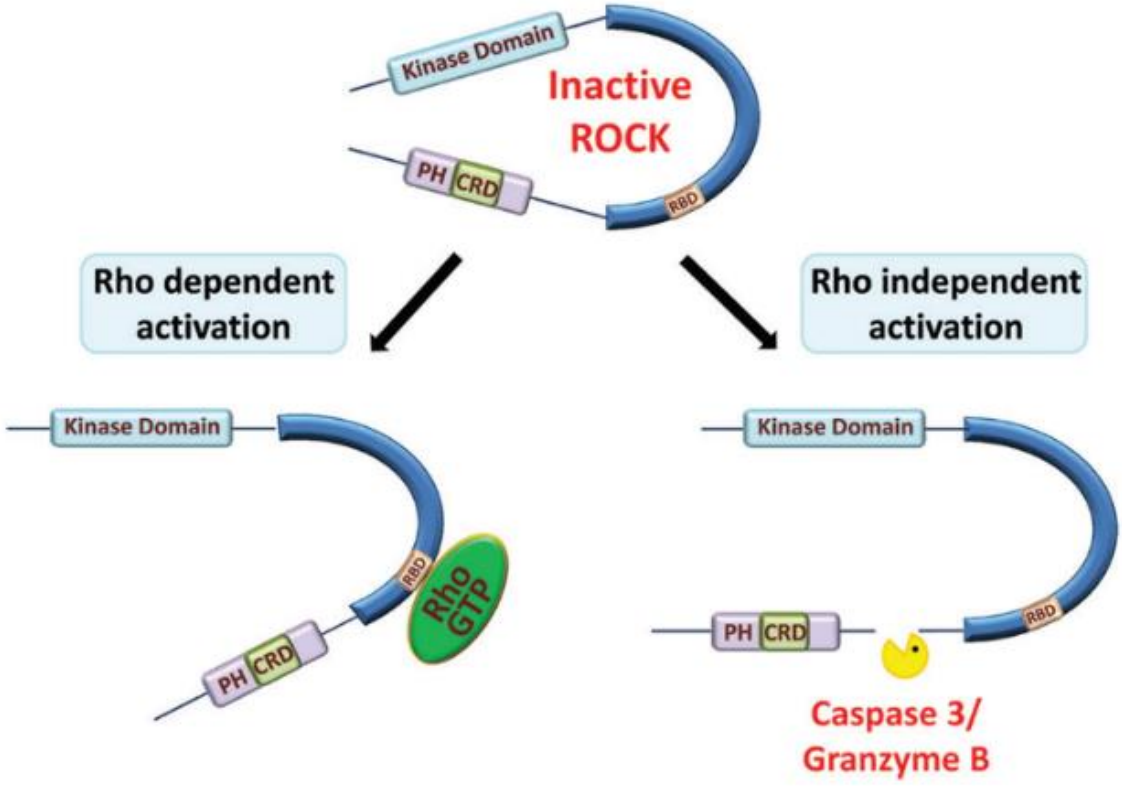

Figure 3: ROCK activation. When Rho GTPase binds to RBD stops the auto-inhibitory regulation. ROCK can also be activated by caspase 3 / granzyme B action. Taken from Julian & Olson, 2014.

When ROCK proteins are activated, they phosphorylate different downstream targets implicated in many cellular processes and due to the high similarity between their kinase

domains, both could have numerous phosphorylation substrates in common. There are two activation ways: independent and dependent (**Figure 3**). The carboxyl-terminal region acts as an auto-inhibitory region keeping it inactive. This negative regulation is disrupted by the association of an active Rho GTPase to the RBD. ROCK may also be activated by the elimination of its carboxyl-terminal through the action of caspase 3 for ROCK1 or granzyme B for ROCK2 (Julian & Olson, 2014).

Curiously, crystal structure observations revealed that their kinase domains are still catalytically competent while being unphosphorylated. This means that, in contrast with other AGC kinases, the RBD is enough to activate the protein (Jacobs et al., 2006). Nevertheless, other kinases can phosphorylate other regions regulating ROCK signalling or subcellular localization. Moreover, although ROCK is usually activated by Rho proteins, it can be inactivated by other GTP-binding proteins like Gem or Rad1 (Ward et al., 2002).

RhoA/ROCK pathway in axon morphogenesis

First time Rho activation was inhibited to study axon growth it was done by using C3 transferase (C3) from *Clostridium botulinum*. C3 showed the capability of promoting optic nerve axons regrowth in the mouse optic nerve crush (ONC) model (Lehmann et al., 1999). After this research, the implication of Rho GTPases in axon growth has been widely studied in several diseases such as spinal cord injury (SCI) (Hu & Selzer, 2017), stroke (Sladojevic, Yu, & Liao, 2017) or neurodegenerative diseases (Jan Christoph Koch et al., 2018). In this way, Rho GTPases have been identified as critical regulators of axon morphogenesis by promoting or inhibiting growth axon depending on the effector mDia or ROCK respectively (Hall & Lalli, 2010) (**Figure 4**).

Glial scar formed after a stroke is characterised by the main presence of reactive astrocytes. Despite producing growth-promoting molecules, they also produce proteoglycans which act as inhibitory extracellular matrix molecules. Four types of them are generated by the reactive astrocytes depending on the composition of the repeating disaccharide, being chondroitin sulfate proteoglycans (CSPGs) those who are involved in inhibiting axon regeneration (Fujita, Yamashita, & Bowerman, 2014). The secretion of CSPGs (aggrecan, brevican, neurocan, NG2, phosphacan, and versican) by reactive astrocytes starts immediately after injury and persists for a long period (Tang, Davies, & Davies, 2003). Some studies have shown genetic deletion of the CSPGs membrane receptors PTPσ (Shen et al., 2009), LAR (Fisher et al., 2011) and NGR1/3 (Dickendesher et al., 2012) enhances axon and neurite growth. However, the knock-out of one of the NGR1/3 is not enough, both must be deleted to see the axon-growth-promotion phenotype, which means their function is probably redundant (Fujita et al., 2014).

ROCK may also be activated by Nogo via the trimeric NGR1/p75/Lingo1 receptor complex or by binding of ephrin-A (Wahl, Barth, Ciossek, Aktories, & Mueller, 2000), semaphorin-3A and semaphorin-4D to their receptors (Figure 4).

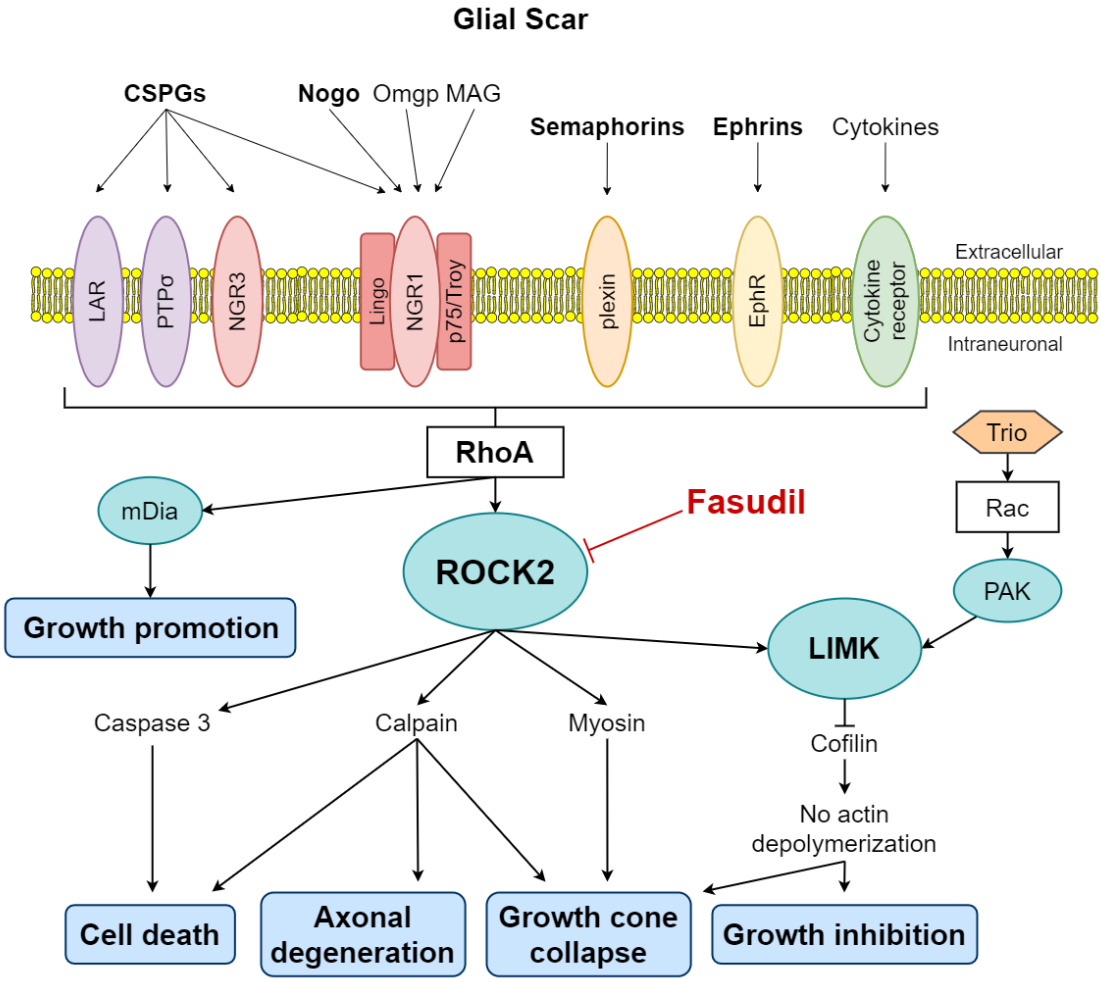

Figure 4: ROCK upstream and downstream regulation scheme. LAR, PTPσ and NGR1/3 receptors transduce CSPGs-mediated inhibition of axon growth through Rho/ROCK pathway. Nogo, semaphorins or ephrins can also activate ROCK by binding to their correspondent receptors. RhoA may promote or inhibit growth axon depending on the effector mDia or ROCK. When ROCK activates LIMK, cofilin is inactivated and, consequently, the actin depolymerization process needed for axon outgrowth is also inhibited. Myosin II activity is also heightened by ROCK resulting in growth cone collapse. ROCK is involved in other damaging processes like apoptosis and axonal degeneration.

Although ROCK is involved in several neuron damaging processes such as cell death, axonal degeneration, growth inhibition or growth cone dynamics, a well-known downstream target of ROCK2 is LIM domain kinase (LIMK), whose activation results in cofilin phosphorylation and its consequent inactivation. When cofilin is activated it acts

by depolymerizing actin filaments, a necessary process for the extension of the actin-cytoskeleton (J C Koch et al., 2014). Alternatively, LIMK can be also activated through Trio/Rac/PAK/LIMK (Hall & Lalli, 2010) as it is showed in **Figure 4**.

Growth cone dynamics are also very important in axon outgrowth. This dynamic is consequence of an extrusion of filopodia and lamellipodia (two types of actin-based membrane protrusions) which is constant and seemingly stochastic (Giniger, 2002). The lamellipodia is a short and branched actin filament network whose main function is movement, whereas filopodia samples the extracellular environment. While *in vivo* growth cone shows an amoeba-like motility, *in vitro* shows a flat and fan-like shape with a peripheral (actin-rich due to the presence of filopodia and lamellipodia) and a central (microtubule-concentrated) region. The transition zone between these mentioned regions seems to contain the actomyosin contractile structures, which is involved in important processes as the regulation of actin and microtubule of the growth cone, included the actin reward flow and the microtubule network maintaining (Omotade, Pollitt, Zheng, & Zheng, 2017).

Two models have been described to explain the role of Rho GTPases in the growth cone guidance. On the one hand, in an instructive model, Rac or Cd42 are activated by attractive guidance cues promoting growth cone advance. Whereas Rho is activated by repulsive cues resulting in the inhibition of axon outgrowth or inducing its retraction. On the other hand, in a permissive model, Rho GTPases would be involved in providing the dynamic actin structures, but the growth cone advance or retraction would be mediated independently of Rho GTPases by signals that regulate the cytoskeleton (Dickson, 2001). However, many studies have reported the implication of Rho GTPases in the growth cone guidance, although this does not discard the possibility of the coexistence of both models.

The inactivation of cofilin activity, and the consequent inhibition of the actin depolymerization, through Rho/ROCK/LIMK explained above is an example of the implication of Rho in the growth cone collapse. Moreover, when ROCK phosphorylates the regulatory myosin light chain (MLC) and inhibits myosin light chain phosphatase (MLCP), contractility is activated. This results in a higher myosin II activity (**Figure 4**), which increases retrograde flow and reduces leading edge protrusion and, consequently, promotes the growth cone collapse (Gomez & Letourneau, 2014).

Finally, although the relations between the pathways are not completely clear, RhoA/ROCK seems to mediate caspase-3 dependent apoptosis (Hannan et al., 2016) and the downregulation of ROCK2 results in a decreased caspase-3 and calpain activity. This last one is implicated in cell death, axonal degeneration, and growth cone collapse (J C Koch et al., 2014; To, Church, & O'Connor, 2008).

Curcumin

Curcumin is a natural and non-toxic polyphenol widely consumed in Asia as a cooking spice which has an important neuroprotective activity (Bhat et al., 2019). The origin of this could be the upregulating sirtuin-1 (SIRT1) mediated by curcumin, as SIRT1 has an important role in cellular metabolism and in oxidative stress protection (Zendedel, Butler, Atkin, & Sahebkar, 2018).

Moreover, curcumin has shown beneficial effects in different brain disorders including stroke, either to prevent it or to treat it. Curcumin may prevent stroke due to its capability of free radical scavenging and the inhibition of the increase in nitric oxide synthesis and lipid peroxidation levels (Bhat et al., 2019). Its protective activity could also be due to the epigenetic modulation action, as curcumin seems to be an epigenetic agent which could reverse epigenetic alteration and be useful in the prevention of stroke (Kalani, Kamat, Kalani, & Tyagi, 2015). Curcumin also seems to be useful in the treatment, because of its regulatory effect on microglial responses, which promotes M2 microglial polarization and inhibits microglia-mediated pro-inflammatory responses. Thus, ischemic stroke-induced brain damage can be reduced by curcumin (Z. Liu et al., 2017)

However, its low solubility, bioavailability, and pharmacokinetic profile raise doubts about its usefulness (Meo, Margarucci, Galderisi, Crispi, & Peluso, 2019). Accordingly, the neuroprotective effect seems to be consequence of the gut microbiota-brain axis, which stablishes a relationship between gut microbiota and brain through neuroanatomical pathways, the neuroendocrine-hypothalamic-pituitary-adrenal axis, neurotransmitters and neural regulators synthesized by intestinal bacteria and the intestinal mucosal and blood-brain barriers (Wang & Wang, 2016).

Microbiota-gut-brain axis

Microbiota-gut-brain axis is a reflex neuronal network which establishes a bidirectional communication system between both organs. Afferent and efferent neurons are implicated in these connecting neuronal pathways proceeding through the parasympathetic (vagal) and sympathetic (splanchnic and pelvic spinal pathways) branches of the autonomic nervous system (ANS). The hypothalamic-pituitary adrenal (HPA) axis takes part in this communication as the release of corticotrophin-releasing factor (CRF) promotes the production of adrenocorticotropic hormone (ACTH) by the pituitary gland and consequently, an increase in cortisol. The enteric nervous system (ENS) is also implicated, as it transmits the information received from the ANS to the gastrointestinal tract. In this way, metabolites generated by the saprophytic microbiota such as short chain fatty acids (SCFAs) may stimulate the production of several neuropeptides by the enteroendocrine cells (EECs) of the gut epithelium. Thus, intrinsic

ENS neurons or extrinsic vagal innervation could be affected by these neuropeptides (Baj et al., 2019). In summary, as **Figure 5** shows in a simple scheme, gut may affect the brain through neurotransmitters and SCFAs produced by the microbiota and, conversely, the hypothalamus-pituitary-adrenal axis may affect immune cells and the consequent cytokine secretion (gut and systemically), gut permeability and microbiota composition (Cryan & Dinan, 2012).

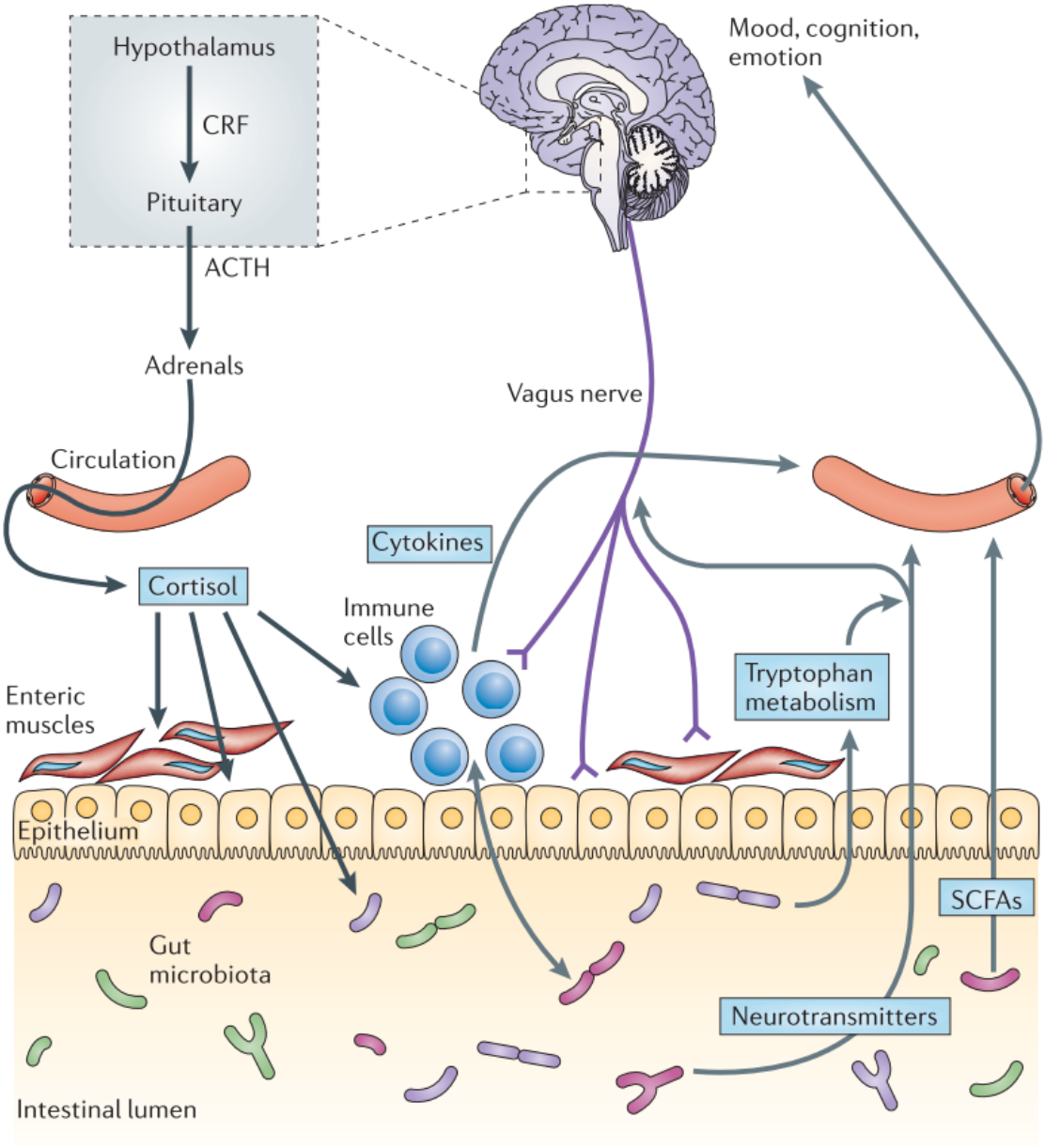

Figure 5: Microbiota-gut-brain axis scheme. Signals can be sent to the central nervous system (CNS) and to the enteric nervous system (ENS) by the microbiota through endocrine, immune, metabolic and neuronal pathways. Gut permeability and barrier function may be altered by cortisol changing gut microbiota composition. The gut microbiota and probiotic agents can also interfere on circulating cytokines affecting the brain function. Taken from Cryan & Dinan, 2012.

Although the exact mechanism of this established communication has not been completely understood, several studies have shown the implication of the microbiota-gut-brain axis in neurodegenerative diseases such as Parkinson (Mulak & Bonaz, 2015), Alzheimer, multiple sclerosis or amyotrophic lateral sclerosis (Quigley, 2017). It could even be involved in neurological disorders like autism (Mangiola et al., 2016) or depression (Zalar, Haslberger, & Peterlin, 2018).

AIM

To sum up the introduced before, on the one hand, inhibiting ROCK is a very interesting approach for promoting axon outgrowth after an ischemic stroke. In fact, lots of inhibitor drugs have been developed as ROCK is implicated in several diseases such as glaucoma, cancer or even psoriasis (Feng, LoGrasso, Defert, & Li, 2016). Accordingly, we strongly believe that Fasudil is a good choice because it has already shown positive effects in acute ischemic stroke and its use for 25 years for vasospasm treatment is signal that it is a safe drug. On the other hand, curcumin has multiple benefits in different neurological disorders included stroke. Moreover, this work is the product of a collaboration with Prof. Victoria Moreno whose group carried out a research testing these compounds in combination in spinal cord injury.

Thus, in this work we propose the administration of Fasudil and curcumin in combination because of their regenerative and neuroprotective effects respectively to treat stroke with the following objectives:

- Determination of the best Fasudil concentrations and conditions *in vitro*.
- Combination assays *in vivo*.

Unfortunately, the extraordinary quarantine situation due to COVID-19 has not allowed the realization of the combination assays, so only the first objective has been accomplished and the following results correspond to what has been done to date.

MATERIALS AND METHODS

Primary neuronal culture

Our experiments have been done *in vitro* using primary cell cultures of cortical neurons electroporated to allow observation. The procedure followed to carry out this process is described below.

Plasmids and maxiprep

Two plasmids were used for cell electroporation: pLenti-Lifeact- tdTomatod bought to Addgene (Addgene plasmid #64048; http://n2t.net/addgene:64048; RRID: Addgene_64048) and developed by Lim et al., 2015; and a plasmid loaned by colleagues from the research centre which express GFP constitutively.

A maxiprep had to be done for DNA amplification and purification. First, a preinoculum was performed by scratching the bacteria stored in a -20 ºC freezer with a pipette tip. Then, the obtained bacteria were introduced in a 1mL Eppendorf containing 1mL of LB-ampicillin medium in sterile conditions. This was incubated for 1-2 hours at 37 ºC and 175 speed in an orbital shaker. Time passed, the preinoculum was transferred to a one-litre flask with LB-ampicillin medium in sterile conditions and incubated on the same conditions for 16-20 hours. Finally, maxipreps were done using a commercial kit bought to NZYtech (Ref. MB051) and following the provided protocol. Purified DNA was measured in a Nanodrop spectrophotometer to prepare a 1 µg/µL aliquot and both stock and aliquot were stored at 4 ºC.

LB-ampicillin medium was prepared by mixing 10 g of sodium chloride, 10 g of tryptone and 5 g of yeast extract in 1L of Milli-Q H_2O. After being autoclaved 1mL of ampicillin (of 1000X aliquots) was added to the medium.

Animals, dissection and disaggregation

Cortical neurons used for cell culture were obtained from embryos brains of Crl:CD1(ICR) strain at the 15^{th} day of gestation (E15). Spanish National Guide for the Care and Use of Experimental Animals (Real Decreto 53/2013) was respected in all procedures as well as the Animal Care Committee of the Principe Felipe Research Centre.

Before cell culture day it is important to anticipate how many plates will be needed, as coverslips to 12 well plates or 60 mm plates have to be treated with poly-L-lysine (Sigma Ref. P2636). To treat coverslips or plates, they had to be washed previously with ethanol 70% and let dry. Stock poly-L-lysine is 5 mg/mL in water and a solution of 0.1mg/mL in PBS1X has to be prepared. Then, coverslips can be treated by putting 200 µL of the poly-

L-lysine solution being added drop by drop to form a bubble over the coverslip or, conversely 2.5 mL of the solution to the 60 mm plates. After being minimum 2 hours at 37 ºC in the cell incubator, poly-L-lysine is removed and three washes with Milli-Q H_2O are done. PBS 1X is prepared by mixing NaCl 137mM, KCl 2,7 mM, Na_2HPO_4 10 mM and KH_2PO_4 2 mM in Milli-Q H_2O and adjusting pH to 7.4.

Dissections of embryos were done after sacrificing pregnant females by cervical dislocation and extracting the uterus. Embryos were decapitated, brains extracted and cortex without other traces of tissue were obtained. Meninges were carefully removed, as they are toxic for the cortical neuronal culture and clean cortices were moved to a small petri dish containing cold HBSS 1X (Thermo Fisher Ref. 14175095). This medium was used in all the dissection process.

Table 1: Electroporation conditions programmed to the electroporator and number of non-electroporated and electroporated cells plated per well, as well as number of well per plate and number of plates used.

Electroporation conditions	Length (ms)	V	Interval	N	D. rate	Polarity
Poring pulse	2	175	50	2	10	plus
Transfer pulse	50	20	50	5	40	Plus/minus

Non-electroporated cells/well	Electroporated cells/well	Well/plate	Nº plates
110000	5500	12	6
3000000	555000	1 (60mm plate)	3

Disaggregation process was done as follows. First, tissue was chopped in big chunks which were transferred to a 15 mL tube. After sinking by gravity, dissecting medium was aspirated and prewarmed trypsin (Thermo Fisher Ref. 25300054) added (5 mL for a full litter). This was mixed by tickling once before and during the incubation every 5 minutes which was done at 37 ºC for 15 minutes in the water bath. Trypsin was removed after letting tissue sink by gravity and three washes with 8 mL of warm HBSS 1X were done agitating gently 30 seconds each time. Then, excess of HBSS was removed and 3 mL of prewarm and equilibrated (by storing in the incubator partially opened) MEM (Thermo

Fisher Ref. 11095080) plating medium were added to do a mechanical disaggregation using a p1000 pipette. Finally, 7 mL of MEM were added, and cells were filtered with a cell strainer placed on a 50 mL tube.

Cell plating

Plating protocol starts after transferring 5 mL of filtered cells to a 15 mL tube, doing a centrifugation for 5 minutes at 1100 rpm and resuspending the pellet with 5 mL of Opti-MEM medium (Thermo Fisher Ref. 31985070). After doing this twice, two more centrifugations were done under the same conditions, but this time resuspension was done with the correspondent volume of Opti-MEM to get 1 million cells/mL in electroporation cuvettes assuming 3 million cells are obtained of each embryo. 5 mL of this solution were used to confirm cell concentration on the Neubauer chamber mixing them with Trypan blue in a 1:2 dilution. To electroporation cuvettes were also added 1.7 µg/µL of pLenti-Lifeact- tdTomatod and 2.7 µg/µL of GFP plasmid. After electroporation, conditions of which are shown in **Table 1**, the appropriate volume of cells is plated on plates/wells containing the plating medium equilibrated and prewarmed. To ensure the uniform distribution, plates were moved in two directions: front to back and right to left. Electroporated cells show better adhesion results if they are plated along with non-electroporated cells. **Table 1** shows the number of non-electroporated and electroporated cells plated in the experiments. Finally, plates are incubated for 2-4 hours at 37 ºC, observed under inverted microscope and plating medium is changed to prewarmed and equilibrated neuronal medium. This medium is prepared by mixing 100mL of Neurobasal medium (Thermo Fisher Ref. 21103049), 2 mL of B-27 (Thermo Fisher Ref. 17504044), 0.25 mL of GlutaMAX 200 mM (Thermo Fisher Ref. 35050061) and 1 mL of penicillin-streptomycin 1X.

Compound treatment

Three types of assays have been performed: an acute treatment for 30 minutes of Fasudil was performed to study the effects in axonal growth cones; long treatments for 24 and 48 hours were done to study axonal elongation; and a trypsinization process to induce neurites injury was carried out as a model of injury, trying to emulate stroke damaging, and the subsequent attempt of regeneration using Fasudil in a 24 hours treatment (**Table 2**).

Compound treatment process was done by extracting 700 µL/well of 12 well plates and saving them in a 15 mL tube which it will be called “conditioned medium” from now on. Then, the remaining medium was aspired sequentially by rows (to prevent cells from

drying out) and 400 µL/well of the conditioned medium saved were added. This was done to make sure we have the same volume in all the wells, as some medium is evaporated in the incubator. Then 100 µL/well of Fasudil were prepared and prewarmed before being added to wells. Fasudil preparation was done by adding the corresponding volume of the drug to the necessary conditioned medium volume keeping in mind the final concentration in 500 µL/well and the different concentrations desires: control (only conditioned medium), 50 µM, 100 µM and 200 µM.

Table 2: This table shows the four types of experiments which have been done, as well as the day Fasudil was added, the day fixation was done and the duration of the treatment of each experiment.

Experiment	Treatment day	Fixation day	Treatment duration	Nº of plates
Growth cone assay	D3	D3	30 min.	1
Axonal elongation assay 24 h	D3	D4	24 h.	3
Axonal elongation assay 48 h	D3	D5	48 h.	2
Axonal injury model	D5	D6	24 h.	3

Fixations were done to interrupt treatment and to observe the effect of Fasudil at these points: after 30 minutes, after 24 hours and after 48 hours. In this work, PFA 4% has been used as a fixative, since many studies show that it allows a greater detection of proteins and in their correct location, as well as a lower decrease of fluorescence compared to the use of other fixatives such as alcohols (Stadler, Skogs, Brismar, Uhlén, & Lundberg, 2010). Fixations were performed by aspiring the medium and adding 800 µL/well of PFA 4% for 10 minutes and doing three washes after with PBS 1X.

To prepare 100 mL of PFA 4%, 70mL of Milli-Q H_2O are boiled in a beaker before putting it on the magnetic stirrer and 4 g of paraformaldehyde are added next. Drops of NaOH can be added if PFA does not dissolve until it does. Then, the beaker is put on ice and 10 mL of PBS 10X are added. Once it is cold Milli-Q H_2O is added up to 100 mL and the solution is filtered.

Trypsinization

Before compound treatment, to see the Fasudil effect on damaged neurons, trypsinization was performed on cells in 60mm plates to subject the cells to stress and damage the neurites to simulate what happens during a stroke, generating our proposed injury model.

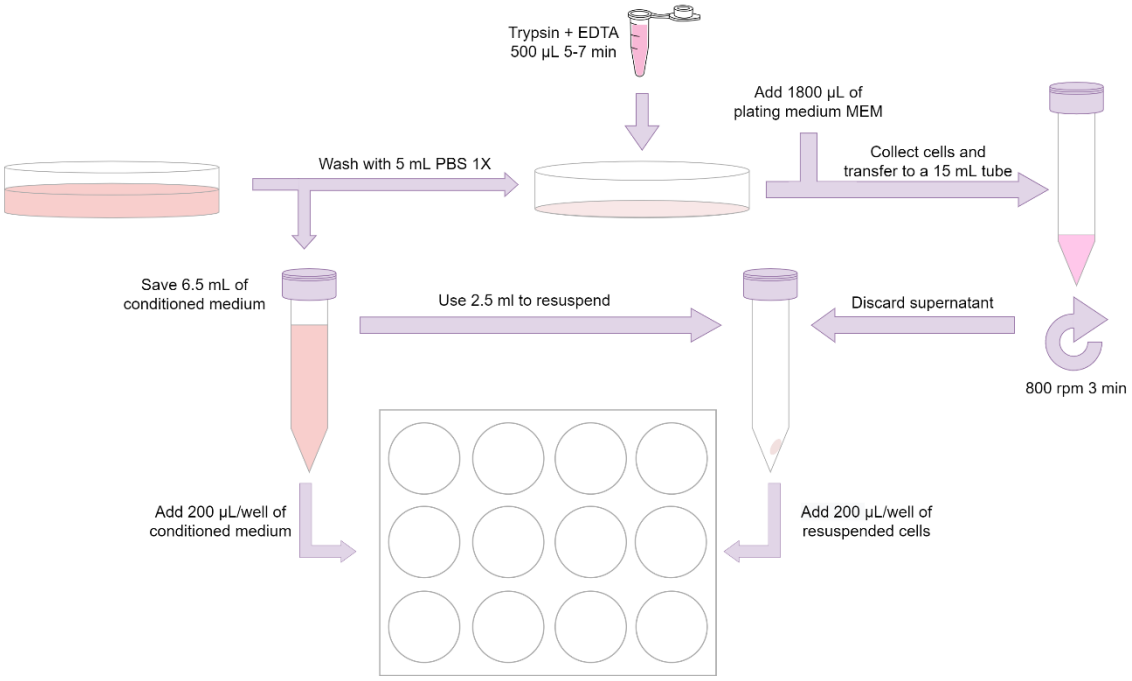

Figure 6: Protocol scheme of trypsinization process done to damage neurites.

Trypsinization process was done at 5th day post culture (D5) as follows. First, 6.5 mL of de medium was extracted and collected and saved in a 15 mL tube (conditioned medium). Then, a wash was done by adding 5 mL of PBS 1X to the 60 mm plate and then aspired. After adding 500 µL of prewarmed trypsin with EDTA, plate was incubated at 37ºC in the cell incubator for 5-7 minutes. Cells were carefully detached by adding 1800 µL of plating medium (MEM) and moving up and down with the p1000 pipette. After collecting this in a 15 mL tube, a centrifugation for 3 minutes at 800 rpm was done. Supernatant was discarded and pellet was resuspended with 2.5 mL of conditioned medium saved before. Then, 200 µL/well of resuspended cells were added to a 12 well plate with coverslips treated previously with poly-L-lysine. Finally, 200 µL/well more were added of conditioned medium. Plate was incubated for 2 hours in the cell incubator before proceeding to the compound treatment to let cells settle and adhere. A scheme of the trypsinization process is showed in **Figure 6**. From now on, compound treatment process

was done to damaged cells of the injury model in the same way as the non-stressed cells as it has been described before.

Immunofluorescence

Immunofluorescence were done to the previously fixated cells in order to increase the fluorescence signal and sensitivity.

First, a permeabilization to allow the penetration of the antibodies into the cells was done by adding 400 µL/well of PBS 1X with Triton X-100 0.1%. After a fast wash and two more of 5-10 minutes with PBS 1X, 300 µL/well of blocking solution (PBS 1X with BSA 2%) were added for 30 minutes at room temperature (RT). Primary antibody anti-GFP in chicken (Aves Labs Ref. GFP-1010) at 1/600 dilution was added and incubated for 2 hours at RT in a wet chamber. After three washes of 10 minutes with PBS 1X, secondary antibody anti-chicken in goat (Thermo Fisher Ref. A-11039) at 1/500 dilution and DAPI 1/2000 was added and incubated for 1 hour at RT and darkness. Finally, coverslips were washed three times with PBS 1X for 10 minutes and mounted on slides using Mowiol mounting medium.

Mowiol medium is prepared by placing 6 g of glycerol in a 50 mL tube, 2.4 g of Mowiol stirring thoroughly and 6 mL of distilled water and leaving it for 2 hours at RT. After time passed, 12 mL of 0.2 M Tris (pH 8.5) are added and incubated at approximately 53ºC until Mowiol has dissolved, which usually takes several hours. Finally, solution is clarified by centrifugation at 4000-5000 rpm for 20 minutes and supernatant is transferred into glass vials with screw caps. This solution is stable at -20˚C for up to 12 months.

Image and data acquisition

Images were acquired with a fluorescence microscope to GFP observation. They were acquired with a 2560x1920 resolution, 16 bits and grey scale. In all experiments, photos of each coverslip in three random areas were taken with 10X objective of DAPI and GFP to have representative photos of the cell culture.

As 30 minutes of treatment is not time enough to see an axon outgrowth, we analysed this experiment observing the growth cone. Accordingly, these images of acute experiment were done with 63X oil immersion objective to take photographs of this structure, while images of the rest of experiments were done with 10X objective to observe the full length of the axon.

Images were analysed with Fiji (ImageJ). First, images were processed by removing the scale (to have the scale in pixels instead of inches) adding a Fire LUT and editing brightness and contrast to allow a better observation of growth cones and axons.

Growth cones were analysed by creating a square of 150x150 px and saving it as a region of interest (ROI) to measure the same area in all cones. Threshold tool was used to make a binary image adjusting to the cone shape. Finally, magic wand was used to select the shape and measuring the area and perimeter of the growth cone (**Figure 7-A**).

A **B**

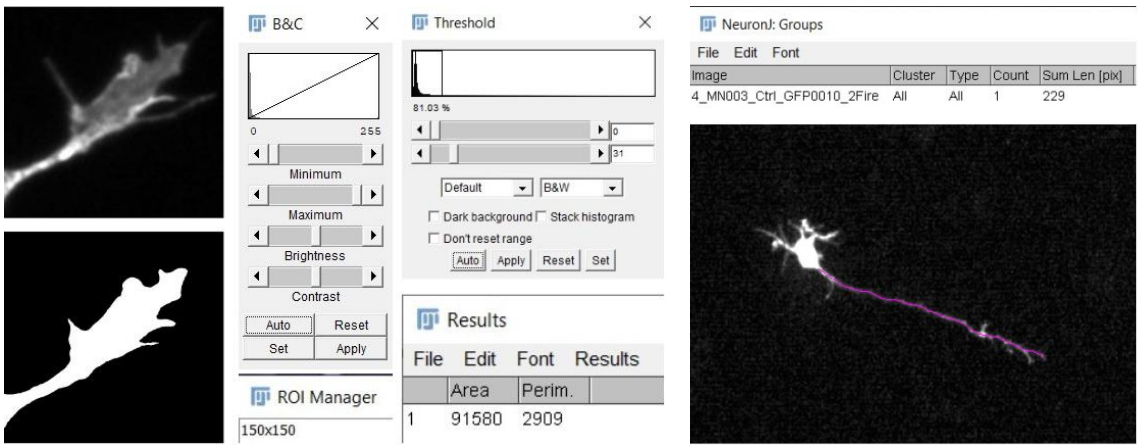

Figure 7: A) Growth cone images analysis. After adjusting brightness and contrast and select a 150x150 px ROI, threshold was modified to obtain the lower left image. White shape was selected with the magic wand and the area and perimeter results are shown. **B)** Axonal length images analysis. After adjusting brightness and contrast in the same way as in growth cone images, NeuronJ plugin was used to draw the axons and length of the tracings were measured.

Axonal lengths were analysed using NeuronJ plugin (Meijering et al., 2004) of Fiji and "add tracing" and "measure tracing" tools were used to draw the axons and measure its length, respectively and then, "make snapshot" tool was used to save each tracing (**Figure 7-B**).

All measures (areas, perimeters and lengths) were saved in excel files for the subsequent data analysis.

Data analysis

Data was analysed with programming language R in RStudio environment. R is a programming language for statistical analyses and one of the most used tools for this aim. Also, as part of the GNU project, it is shared open-source. Some of the multiple advantages of using a programming language are transparency, automation of repeated analyses, troubleshooting and reproducibility (Jalal et al., 2017).

First, data was normalised to decrease variability between different cultures, as some experiments were done more than once (see Nº of plates in **Table 2**). This was done by dividing all measures by the average of their respective control. Moreover, excel files were saved in csv (comma-separated values) format to use them in RStudio.

While *t*-test is used to compare two populations or groups, Analysis of Variance (ANOVA) is used with more than two populations. Accordingly, ANOVAs were done to study the significance between our different groups: control, 50 µM, 100 µM and 200 µM. Then, Tukey's Wholly Significant Difference (WSD) test was used as it is the most appropriate with small samples (Park, Cho, & Ki, 2009).

The R code used was as follows:

```
anova <- aov(normalised_length~condition, data = experiment)
TukeyHSD(anova)
```

RESULTS

Growth cone assay

Primary cortical cultures were treated with Fasudil to see the effect of the drug with different concentrations and after different treatment durations. Since, at first, we were interested in determinate which concentrations and treatment durations worked better in CD1 strain before testing Fasudil in the injury model.

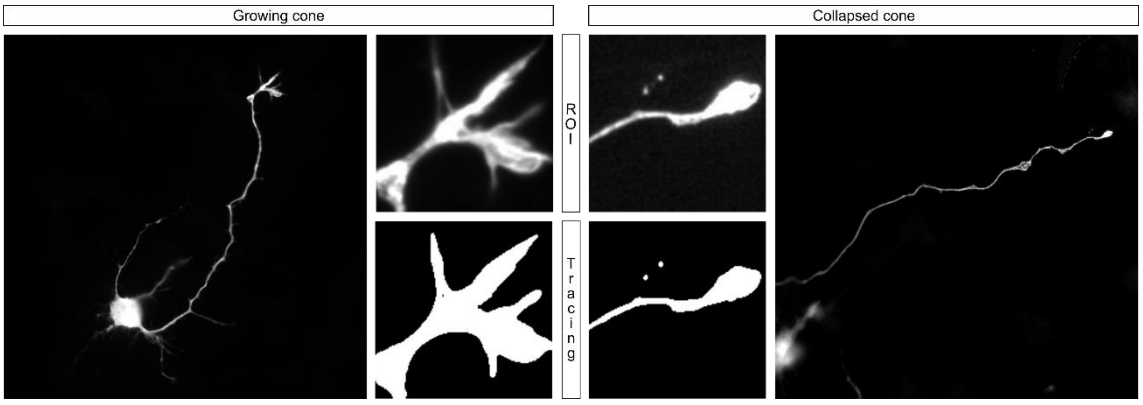

Figure 8: Representative image of a growing cone and a collapsed cone. ROI images are the 150x150px square used in all images to always measure the same section of the growth cone. Tracing represent the binary images done to measure areas and perimeters in ImageJ.

Acute treatment at D3 for 30 minutes was analysed by measuring area and perimeter of growth cones, as 30 minutes is not time enough to see an axon outgrowth. Approximately between 20 and 30 pictures of each coverslip (60-90 per condition) were taken to be analysed later. However, we did not see significant differences. (**Table 3**). All ANOVAs and Tukey's test results are in supplementary material in annexe. For this reason, we decided doing longer treatments and measuring axonal lengths.

Table 3: Acute treatment results. Means, standard deviations and p-values respect to control of areas and perimeters measured of each condition and number of measures. P-values 50 µM – 100 µM see **Figure Suppl. 1**.

	Area			Perimeter			
Condition	Mean (μ^2)	σ	p-value	Mean (µ)	σ	p-value	N
Control	1550.48	1396.47	-	265.58	120.23	-	59
Fasudil 50 µM	1487.72	1297.67	0.86	286.99	154.03	0.22	89
Fasudil 100 µM	1632.26	1360.90	0.79	284.86	141.70	0.31	77

Axonal elongation assays

Long treatment assays were analysed by measuring axonal lengths, as conversely to acute treatment, 24 and 48 hours are enough to see axon outgrowth. In the same way that acute treatment, drug was added in these ones at D3.

Table 4: Number of measures of each condition in each assay, as well as the number of measures per plate (see Nº of plates in **Table 2**). Although injury model was done trice, only two plates were finally measured due to problems in the culture.

	N			N / Nº plates		
	Control	50 µM	100 µM	Control	50 µM	100 µM
24 hours	614	355	261	204.7	118.3	87
48 hours	396	308	128	198	154	64
Injury model	318	182	167	159	91	83.5

Unlike the growth cone assay, the pictures of which were taken with the 63x objective, axonal elongation assay pictures were taken with the 10x one. Thus, as many photos as necessary were taken to photograph the entire coverslips surface. Since in each picture there are several neurons, as many measures as were possible were taken of all neurons with a visible axon which could be traced, since the crossover of several axons makes it difficult to trace them. Therefore, we can get an idea of the number of neurons of each condition according to the number of measurements, taking into account that with a higher concentration of the drug, the longer the axons are and the more difficult the tracing is due to crossing. As it can be observed in **Table 4**, approximately 200 control neurons were measured in axonal elongation assays, with 50 µM concentration measures are less than 200 and more than 100 and, with 100 µM concentration less than 100 neurons were measured.

24 hours treatment results show a clear increase (p-values < .001) in axonal length except in 200 µM concentration case where lengths were barely longer than control lengths as it can be observed in **Figure 9** and **Figure Suppl. 2**. Accordingly, 200 µM concentration seems to be toxic, which had already been reported by Prof. V. Moreno group who tested Fasudil and curcumin in spinal cord injury (Benedetta Calabrese, 2017). Because of this, we did not use 200 µM concentration in 48 hours treatment. Moreover, while 24 hours treatment was done thrice, 48 hours treatment was done twice (Nº of plates in **Table 2**) as we had already analysed 24 hours treatment and we had seen how reproducible our

results were. In the same way as 24 hours treatment, 48 hours treatment also shows an increase in axonal length with p-values <.001 as shows (**Figure 10** and **Figure Supple 4**).

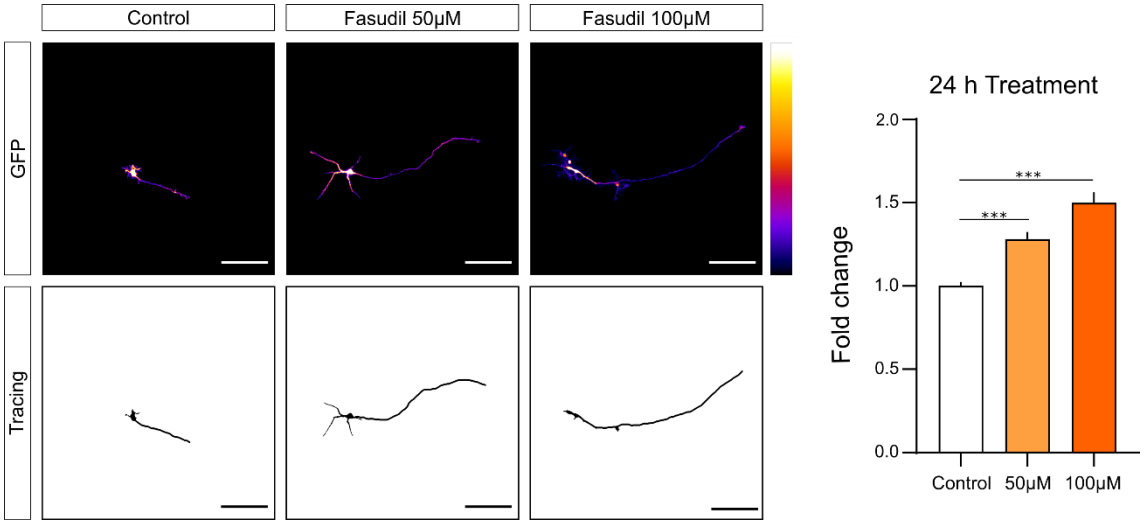

Figure 9: 24 hours results: a representative image of each condition. GFP images are processed removing background, to see them with background see **Figure Suppl. 2**. Colour bar represents GFP signal. Tracing correspond to the length measured in ImageJ and the drawn soma. Scale bars correspond to 100 µm. Bar plot represents normalised mean respect to control. Only p-values respect to control are indicated, to see p-value 50 µM – 100 µM see **Figure Suppl. 3**. *** indicates p-value <.001.

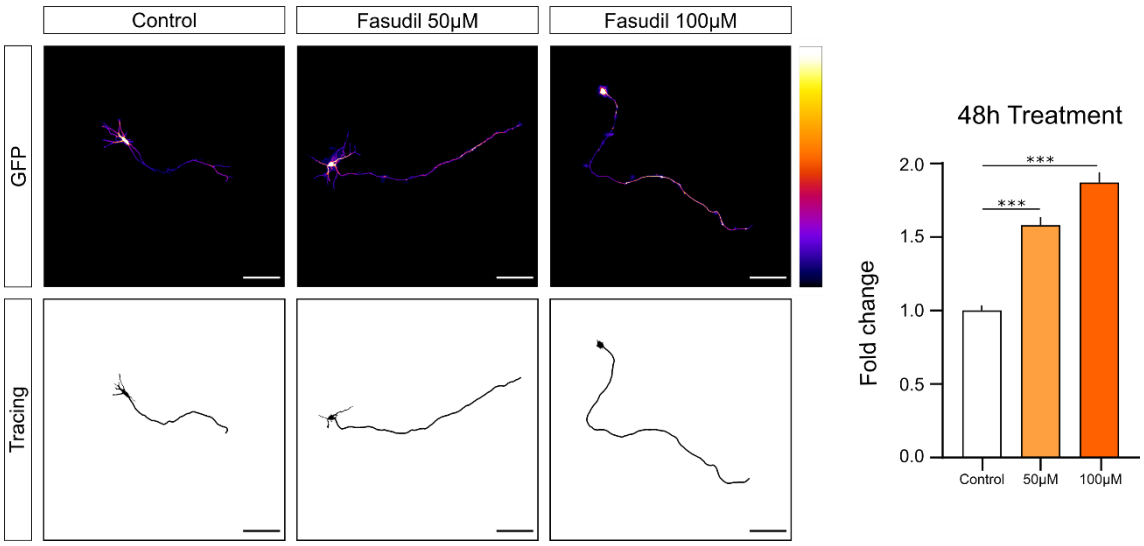

Figure 10: 48 hours results: a representative image of each condition. GFP images are processed removing background, to see them with background see **Figure Suppl. 4**. Colour bar represents GFP signal. Tracing correspond to the length measured in ImageJ and the drawn soma. Scale bars correspond to 100 µm. Bar plot represents normalised mean respect to control. Only p-values respect to control are indicated, to see p-value 50 µM – 100 µM see **Figure Suppl. 5**. *** indicates p-value <.001.

Axonal injury and regeneration model

Trypsinization process was done to emulate neurites injury in ischemic strokes. After this stress situation, culture was let rest for 2 hours before adding Fasudil, whose treatment lasted 24 hours.

This was also analysed by measuring axon lengths, measures are shown in **Table 4**. Although this assay was done trice (**Table 2**), one of them was discarded due to the high mortality rate, which is signal of some problem in the culture during the process. Since these neurons have undergone a process of damage in axons, measures are shorter than non-stressed neurons. However, Fasudil was able to promote a significant outgrowth ($p<.001$) in 24 hours with both 50 µM and 100 µM concentrations as it is showed in **Figure 11**.

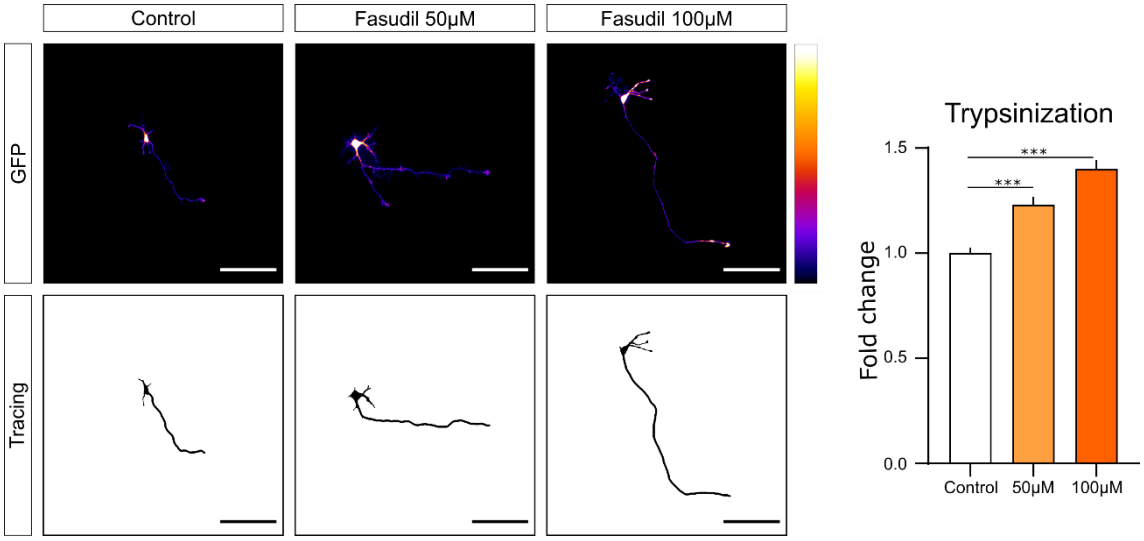

Figure 11: Axonal injury and regeneration model results: a representative image of each condition. GFP images are processed removing background, to see them with background see **Figure Suppl. 6**. Colour bar represents GFP signal. Tracing correspond to the length measured in ImageJ and the drawn soma. Scale bars correspond to 100 µm. Bar plot represents normalised mean respect to control. Only p-values respect to control are indicated, to see p-value 50 µM – 100 µM see **Figure Suppl. 7**. *** indicates p-value <.001.

DISCUSSION

Stroke was, globally, the second largest cause of death in 2016 (Johnson et al., 2019). Although incidence is higher in men, women are more likely to suffer more severe strokes and, subsequently, higher mortality and disability rates (Rodgers, 2013).

After a stroke, it is important to promote regeneration and neuroplasticity of penumbra zone neurons in order to recover ischemic core and, accordingly, develop strategies to achieve this recovery. Multiple axon guidance molecules are involved in negative processes to neuronal survival and plasticity. The activation of RhoA is clearly associated with them, as multiple downstream elements of the pathway are involved in processes such as growth cone collapse, growth inhibition, axonal degeneration or even cell death. Thus, multiple RhoA inhibitors have been tested as promising new therapies in stroke, as well as some inhibitors of upstream elements of the pathway such as Sema3A inhibitor (Wu et al., 2005). We bet on Fasudil as its use in vasospasm gives us useful information about doses or adverse effects in order to be used as a stroke treatment.

Despite the fact that we expected to see a higher proportion of growing cones than collapsed cones in the first assay, this could be due to the fact that it is a very dynamic structure which is in constant protrusion and collapse (Ye, Qiu, Gao, Wan, & Zhu, 2019). Nevertheless, it is widely described in literature that ROCK inhibitors increase protrusive activity by increasing the frequency of filopodial and lamellipodial initiation (Fincher, Whiteneck, & Birgbauer, 2014; Loudon, Silver, Yee, & Gallo, 2006) promoting a higher probability of finding growing cones than collapsed cones. In this way, probably our incapability to obtain significant results measuring areas and perimeters of growth cones is due to limitations in our approach.

On the other hand, our long treatment assays, carried out for 24 and 48 hours, show a significant increase in axonal length and, consequently, an axon outgrowth promotion as expected based on the results of several studies and the settled knowledge about the relation between ROCK inhibitors and axon outgrowth (Fujita et al., 2014). This increase with p-values <.001 can be observed with 50 and 100 µM, however, 200 µM concentration seemed to be toxic. This had already been reported by Prof. V. Moreno's group which tested Fasudil and curcumin in spinal cord injury (Benedetta Calabrese, 2017). Because of this, we did not use 200 µM concentration in 48 hours treatment. Although 100 µM concentration induces significant axon outgrowth, somas show a worse appearance, as if they were shrunk and with less neurites, showing an onset of toxicity. Moreover, decreasing neurons measured showed in **Table 4** could indicate a slight toxicity that increases with concentration but it is important to highlight the limitations,

as longer axons are more difficult to trace as they intersect with others, especially those of 48 hours treatment, so maybe the longest lengths are underrepresented.

Trypsinization process, also, has demonstrated to be useful to emulate neurites damaged and to generate an injury model to the subsequent regeneration with Fasudil. Results of this assays also show a significant axon outgrowth with 50 and 100 µM concentrations with p-values <.001 as well as in the non-damaged primary cortical neurons assay. These results are consistent with previous studies where protective effect of Fasudil was tested in neuronal cultures after subjecting cells to a stress situation (Satoh, Kawasaki, Hitomi, Ikegaki, & Asano, 2011). Moreover, Fasudil was added two hours after trypsinization process and Shibuya et al. concluded in 2005 that the best therapeutic window of Fasudil to treat ischemic stroke is within the first 48 hours. Accordingly, our results are not only significant with very low p-values, but also, they show what is expected according to the literature about Fasudil in axon outgrowth and in stroke treatment.

These results will serve to enlarge knowledge about the mechanisms involved in cell death after stroke, and also about the axonal guidance cues as the most responsible for the activation of the pathways implicated in those process, such as RhoA. Promoting neuroplasticity would considerably reduce the disabilities and cognitive impairment which appear after a stroke as a consequence of the loss of synaptically active neurons or inflammatory processes. Finally, the fact that Fasudil is a known drug because of its use in vasospasm brings us closer to a new therapy which would be able to avoid these negative processes triggered after a stroke.

CONCLUSIONS AND FUTURE PERSPECTIVES

In summary, despite we did not see significant results after 30 minutes of treatment studying the areas and perimeters of growth cones, our results show Fasudil promotes axon outgrowth with 50 µM and 100 µM concentrations after 24 hours and 48 hours of treatment in primary cortical cultures. These results are consistent with the results obtained by Prof. V. Moreno group who tested Fasudil and curcumin in spinal cord injury. Therefore, it makes sense that Fasudil shows better therapeutic results in combination with curcumin in ischemic stroke treatment, as we obtained significant results in our injury and regeneration model damaging neurites with a trypsinization process. Moreover, Fasudil has already been shown to be effective alone in a clinical trial in the treatment of acute ischemic stroke (Shibuya et al., 2005).

Thus, in the next future we want to test this combination of Fasudil and curcumin with *in vivo* models, following steps Prof. V. Moreno did in spinal cord injury, as secondary injury mechanisms in stroke are responsible in most cases of cognitive impairment due to process such as inflammation or endothelial dysfunction after stroke.

REFERENCES

Aho, K., Harmsen, P., Hatano, S., Marquardsen, J., Smirnov, V. E., & Strasser, T. (1980). Cerebrovascular disease in the community: results of a WHO collaborative study. *Bulletin of the World Health Organization*, *58*(1), 113–130.

Baj, A., Moro, E., Bistoletti, M., Orlandi, V., Crema, F., & Giaroni, C. (2019). Glutamatergic Signaling Along The Microbiota-Gut-Brain Axis. *International Journal of Molecular Sciences*, *20*(6), 1482. https://doi.org/10.3390/ijms20061482

Benedetta Calabrese, G. (2017). *Inhibition of the Rho / ROCK signalling pathway by a new combination of compounds and its application in spinal cord injury*. Università Degli Studi Di Trieste.

Bhat, A., Mahalakshmi, A. M., Ray, B., Tuladhar, S., Hediyal, T. A., Manthiannem, E., … Sakharkar, M. K. (2019). Benefits of curcumin in brain disorders. *BioFactors*, *45*(5), 666–689. https://doi.org/10.1002/biof.1533

Bos, J. L., Rehmann, H., & Wittinghofer, A. (2007). GEFs and GAPs: Critical Elements in the Control of Small G Proteins. *Cell*, *129*(5), 865–877. https://doi.org/10.1016/j.cell.2007.05.018

Cheng, N. T., & Kim, A. S. (2015). Intravenous Thrombolysis for Acute Ischemic Stroke Within 3 Hours Versus Between 3 and 4.5 Hours of Symptom Onset. *The Neurohospitalist*, *5*(3), 101–109. https://doi.org/10.1177/1941874415583116

Cherfils, J., & Zeghouf, M. (2013). Regulation of Small GTPases by GEFs, GAPs, and GDIs. *Physiological Reviews*, *93*(1), 269–309. https://doi.org/10.1152/physrev.00003.2012

Cryan, J. F., & Dinan, T. G. (2012). Mind-altering microorganisms: The impact of the gut microbiota on brain and behaviour. *Nature Reviews Neuroscience*, *13*(10), 701–712. https://doi.org/10.1038/nrn3346

Dąbrowski, J., Czajka, A., Zielińska-Turek, J., Jaroszyński, J., Furtak-Niczyporuk, M., Mela, A., … Ziemba, A. (2019). Brain Functional Reserve in the Context of Neuroplasticity after Stroke. *Neural Plasticity*, *2019*, 1–10. https://doi.org/10.1155/2019/9708905

Dickendesher, T. L., Baldwin, K. T., Mironova, Y. A., Koriyama, Y., Raiker, S. J., Askew, K. L., … Neurosci, N. (2012). NgR1 and NgR3 are Receptors for Chondroitin Sulfate Proteoglycans. *Nature Neuroscience*, *15*(5), 703–714. https://doi.org/10.1038/nn.3070

Dickson, B. J. (2001). Rho GTPases in growth cone guidance. *Current Opinion in Neurobiology*, *11*(1), 103–110. https://doi.org/10.1016/S0959-4388(00)00180-X

Donnan, G. A., Fisher, M., Macleod, M., & Davis, S. M. (2008). Stroke. *Lancet*, *371*(9625), 1612–1623. https://doi.org/10.1016/S0140-6736(08)60694-7

Dovas, A., & Couchman, J. R. (2005). RhoGDI: multiple functions in the regulation of Rho family GTPase activities. *Biochemical Journal*, *390*(1), 1–9. https://doi.org/10.1042/BJ20050104

Dransart, E., Olofsson, B., & Cherfils, J. (2005). RhoGDIs Revisited: Novel Roles in Rho Regulation. *Traffic*, *6*(11), 957–966. https://doi.org/10.1111/j.1600-0854.2005.00335.x

Duffy, P., Schmandke, A., Schmandke, A., Sigworth, J., Narumiya, S., Cafferty, W. B. J., & Strittmatter, S. M. (2009). Rho-Associated Kinase II (ROCKII) Limits Axonal Growth after Trauma within the Adult Mouse Spinal Cord. *The Journal of Neuroscience*, *29*(48), 15266–15276. https://doi.org/10.1523/JNEUROSCI.4650-09.2009

Feng, Y., LoGrasso, P. V, Defert, O., & Li, R. (2016). Rho Kinase (ROCK) Inhibitors and Their

Therapeutic Potential. *Journal of Medicinal Chemistry*, *59*(6), 2269–2300. https://doi.org/10.1021/acs.jmedchem.5b00683

Fincher, J., Whiteneck, C., & Birgbauer, E. (2014). GPCR cell signaling pathways mediating embryonic chick retinal growth cone collapse induced by LPA and S1P. *Developmental Neuroscience*, *36*(6), 443–453. https://doi.org/10.1159/000364858

Fisher, D., Xing, B., Dill, J., Li, H., Hoang, H. H., Zhao, Z., … Li, S. (2011). Leukocyte Common Antigen-Related Phosphatase Is a Functional Receptor for Chondroitin Sulfate Proteoglycan Axon Growth Inhibitors. *The Journal of Neuroscience*, *31*(40), 14051–14066. https://doi.org/10.1523/JNEUROSCI.1737-11.2011

Fujita, Y., Yamashita, T., & Bowerman, M. (2014). Axon growth inhibition by RhoA/ROCK in the central nervous system. *Frontiers in Neuroscience*, *8*(338), 1–12. https://doi.org/10.3389/fnins.2014.00338

Garcia-Mata, R., Boulter, E., & Burridge, K. (2011). The invisible hand: regulation of RHO GTPases by RHOGDIs. *Nature Reviews Molecular Cell Biology*, *12*(8), 493–504. https://doi.org/10.1038/nrm3153

Giniger, E. (2002). How do Rho family GTPases direct axon growth and guidance? A proposal relating signaling pathways to growth cone mechanics. *Differentiation*, *70*(8), 385–396. https://doi.org/10.1046/j.1432-0436.2002.700801.x

Gomez, T. M., & Letourneau, P. C. (2014). Actin Dynamics in Growth Cone Motility and Navigation. *Journal of Neurochemistry*, *129*(2), 221–234. https://doi.org/10.1111/jnc.12506

Govek, E. E., Newey, S. E., Akerman, C. J., Cross, J. R., Der Veken, L. Van, & Van Aelst, L. (2004). The X-linked mental retardation protein oligophrenin-1 is required for dendritic spine morphogenesis. *Nature Neuroscience*, *7*(4), 364–372. https://doi.org/10.1038/nn1210

Guzik, A., & Bushnell, C. (2017). Stroke Epidemiology and Risk Factor Management. *CONTINUUM: Lifelong Learning in Neurology*, *23*(1), 15–39. https://doi.org/10.1212/CON.0000000000000416

Haga, R. B., & Ridley, A. J. (2016). Rho GTPases: Regulation and roles in cancer cell biology. *Small GTPases*, *7*(4), 207–221. https://doi.org/10.1080/21541248.2016.1232583

Hall, A., & Lalli, G. (2010). Rho and Ras GTPases in Axon Growth, Guidance, and Branching. *Cold Spring Harbor Perspectives in Biology*, *2*(2), a001818. https://doi.org/10.1101/cshperspect.a001818

Hannan, J. L., Matsui, H., Sopko, N. A., Liu, X., Weyne, E., Albersen, M., … Bivalacqua, T. J. (2016). Caspase-3 dependent nitrergic neuronal apoptosis following cavernous nerve injury is mediated via RhoA and ROCK activation in major pelvic ganglion. *Scientific Reports*, *6*(29416), 1–12. https://doi.org/10.1038/srep29416

Hodge, R. G., & Ridley, A. J. (2016). Regulating Rho GTPases and their regulators. *Nature Reviews Molecular Cell Biology*, *17*(8), 496–510. https://doi.org/10.1038/nrm.2016.67

Hou, S. T., Jiang, S. X., & Smith, R. A. (2008). Permissive and Repulsive Cues and Signalling Pathways of Axonal Outgrowth and Regeneration. *International Review of Cell and Molecular Biology*, *267*(08), 125–181. https://doi.org/10.1016/S1937-6448(08)00603-5

Hu, J., & Selzer, M. E. (2017). RhoA as a target to promote neuronal survival and axon regeneration. *Neural Regeneration Research*, *12*(4), 525–528. https://doi.org/10.4103/1673-5374.205080

Jacobs, M., Hayakawa, K., Swenson, L., Bellon, S., Fleming, M., Taslimi, P., & Doran, J. (2006). The Structure of Dimeric ROCK I Reveals the Mechanism for Ligand Selectivity. *The*

Journal of Biological Chemistry, *281*(1), 260–268. https://doi.org/10.1074/jbc.M508847200

Jalal, H., Pechlivanoglou, P., Krijkamp, E., Alarid-Escudero, F., Enns, E., & Myriam Hunink, M. G. (2017). An Overview of R in Health Decision Sciences. *Medical Decision Making*, *37*(7), 735–746. https://doi.org/10.1177/0272989X16686559

Johnson, C. O., Nguyen, M., Roth, G. A., Nichols, E., Alam, T., Abate, D., … Murray, C. J. L. (2019). Global, regional, and national burden of stroke, 1990–2016: a systematic analysis for the Global Burden of Disease Study 2016. *The Lancet Neurology*, *18*(5), 439–458. https://doi.org/10.1016/S1474-4422(19)30034-1

Julian, L., & Olson, M. F. (2014). Rho-associated coiled-coil containing kinases (ROCK), structure, regulation, and functions. *Small GTPases*, *5*(2), 1–12. https://doi.org/10.4161/sgtp.29846

Kalani, A., Kamat, P. K., Kalani, K., & Tyagi, N. (2015). Epigenetic impact of curcumin on stroke prevention. *Metabolic Brain Disease*, *30*(2), 427–435. https://doi.org/10.1007/s11011-014-9537-0

Kalaria, R. N., Akinyemi, R., & Ihara, M. (2016). Stroke injury, cognitive impairment and vascular dementia. *Biochimica et Biophysica Acta - Molecular Basis of Disease*, *1862*(5), 915–925. https://doi.org/10.1016/j.bbadis.2016.01.015

Kim, J.-G., Islam, R., Cho, J. Y., Jeong, H., Cap, K.-C., Park, Y., … Park, J.-B. (2018). Regulation of RhoA GTPase and various transcription factors in the RhoA pathway. *Journal of Cellular Physiology*, *233*(9), 6381–6392. https://doi.org/10.1002/jcp.26487

Koch, Jan Christoph, Tatenhorst, L., Roser, A. E., Saal, K. A., Tönges, L., & Lingor, P. (2018). ROCK inhibition in models of neurodegeneration and its potential for clinical translation. *Pharmacology and Therapeutics*, *189*, 1–21. https://doi.org/10.1016/j.pharmthera.2018.03.008

Koch, J C, Tö Nges, L., Barski, E., Michel, U., Bähr, M., & Lingor, P. (2014). ROCK2 is a major regulator of axonal degeneration, neuronal death and axonal regeneration in the CNS. *Cell Death and Disease*, *5*, e1225. https://doi.org/10.1038/cddis.2014.191

Koh, S.-H., & Park, H.-H. (2017). Neurogenesis in Stroke Recovery. *Translational Stroke Research*, *8*(1), 3–13. https://doi.org/10.1007/s12975-016-0460-z

Lehmann, M., Fournier, A., Selles-Navarro, I., Dergham, P., Sebok, A., Leclerc, N., … Mckerracher, L. (1999). Inactivation of Rho Signaling Pathway Promotes CNS Axon Regeneration. *The Journal of Neuroscience*, *19*(17), 7537–7547.

Lim, C.-Y., Bi, X., Wu, D., Kim, J. B., Gunning, P. W., Hong, W., & Han, W. (2015). Tropomodulin3 is a novel Akt2 effector regulating insulin-stimulated GLUT4 exocytosis through cortical actin remodeling. *Nature Communications*, *6*(1), 1–15. https://doi.org/10.1038/ncomms6951

Liu, J., Wada, Y., Katsura, M., Tozawa, H., Erwin, N., Kapron, C. M., … Liu, J. (2018). Rho-Associated Coiled-Coil Kinase (ROCK) in Molecular Regulation of Angiogenesis. *Theranostics*, *8*(21), 6053–6069. https://doi.org/10.7150/thno.30305

Liu, Z., Ran, Y., Huang, S., Wen, S., Zhang, W., Liu, X., … Watt, D. (2017). Curcumin Protects against Ischemic Stroke by Titrating Microglia/ Macrophage Polarization. *Frontiers in Aging Neuroscience*, *9*(233), 1–10. https://doi.org/10.3389/fnagi.2017.00233

Loudon, R. P., Silver, L. D., Yee, H. F., & Gallo, G. (2006). RhoA-Kinase and Myosin II Are Required for the Maintenance of Growth Cone Polarity and Guidance by Nerve Growth Factor. *Journal of Neurobiology*, *66*(8), 847–867. https://doi.org/10.1002/neu.20258

Mangiola, F., Ianiro, G., Franceschi, F., Fagiuoli, S., Gasbarrini, G., Gasbarrini Francesca Mangiola, A., … Hepatology, T. (2016). Gut microbiota in autism and mood disorders. *World J Gastroenterol*, *22*(1), 361–368. https://doi.org/10.3748/wjg.v22.i1.361

Meijering, E., Jacob, M., Sarria, J.-C. F., Steiner, P., Hirling, H., & Unser, M. (2004). Design and validation of a tool for neurite tracing and analysis in fluorescence microscopy images. *Cytometry*, *58A*(2), 167–176. https://doi.org/10.1002/cyto.a.20022

Meo, F. Di, Margarucci, S., Galderisi, U., Crispi, S., & Peluso, G. (2019). Curcumin, Gut Microbiota, and Neuroprotection. *Nutrients*, *11*(10), 2426. https://doi.org/10.3390/nu11102426

Mulak, A., & Bonaz, B. (2015). Brain-gut-microbiota axis in Parkinson's disease. *World Journal of Gastroenterology*, *21*(37), 10609–10620. https://doi.org/10.3748/wjg.v21.i37.10609

Nakagawa, O., Fujisawa, K., Ishizaki, T., Saito, Y., Nakao, K., & Narumiya, S. (1996). ROCK-I and ROCK-II, two isoforms of Rho-associated coiled-coil forming protein serine/threonine kinase in mice. *FEBS Letters*, *392*(2), 189–193. https://doi.org/10.1016/0014-5793(96)00811-3

Narumiya, S., & Thumkeo, D. (2018). Rho signaling research: history, current status and future directions. *FEBS Letters*, *592*, 1763–1776. https://doi.org/10.1002/1873-3468.13087

Omotade, O. F., Pollitt, S. L., Zheng, J. Q., & Zheng, J. (2017). Actin-Based Growth Cone Motility and Guidance HHS Public Access. *Molecular and Cellular Neuroscience*, *84*, 4–10. https://doi.org/10.1016/j.mcn.2017.03.001

Park, E., Cho, M., & Ki, C. S. (2009). Correct use of repeated measures analysis of variance. *Korean Journal of Laboratory Medicine*, *29*(1), 1–9. https://doi.org/10.3343/kjlm.2009.29.1.1

Puig, B., Brenna, S., & Magnus, T. (2018). Molecular Communication of a Dying Neuron in Stroke. *International Journal of Molecular Sciences*, *19*(9), 2834. https://doi.org/10.3390/ijms19092834

Quigley, E. M. M. (2017). Microbiota-Brain-Gut Axis and Neurodegenerative Diseases. *Current Neurology and Neuroscience Reports*, *17*(12), 94. https://doi.org/10.1007/s11910-017-0802-6

Rodgers, H. (2013). Stroke. In *Handbook of Clinical Neurology* (Vol. 110, pp. 427–433). https://doi.org/10.1016/B978-0-444-52901-5.00036-8

Satoh, S. I., Kawasaki, K., Hitomi, A., Ikegaki, I., & Asano, T. (2011). Fasudil protects cultured N1E-115 cells against lysophosphatidic acid-induced neurite retraction through inhibition of Rho-kinase. *Brain Research Bulletin*, *84*(2), 174–177. https://doi.org/10.1016/j.brainresbull.2010.11.013

Shen, Y., Tenney, A. P., Busch, S. A., Horn, K. P., Cuascut, F. X., Liu, K., … Flanagan, J. G. (2009). PTPσ Is a Receptor for Chondroitin Sulfate Proteoglycan, an Inhibitor of Neural Regeneration. *Science*, *326*(5952), 592–596. https://doi.org/10.1126/science.1178310

Shibuya, M., Hirai, S., Seto, M., Satoh, S. I., & Ohtomo, E. (2005). Effects of fasudil in acute ischemic stroke: Results of a prospective placebo-controlled double-blind trial. *Journal of the Neurological Sciences*, *238*(1–2), 31–39. https://doi.org/10.1016/j.jns.2005.06.003

Shibuya, M., Suzuki, Y., Sugita, K., Saito, I., Sasaki, T., Takakura, K., … Nakashima, M. (1992). Effect of AT877 on cerebral vasospasm after aneurysmal subarachnoid hemorrhage: Results of a prospective placebo-controlled double-blind trial. *Journal of Neurosurgery*, *76*(4), 571–577. https://doi.org/10.3171/jns.1992.76.4.0571

Sladojevic, N., Yu, B., & Liao, J. K. (2017). ROCK as a therapeutic target for ischemic stroke. *Expert Review of Neurotherapeutics*, *17*(12), 1167–1177. https://doi.org/10.1080/14737175.2017.1395700

Stadler, C., Skogs, M., Brismar, H., Uhlén, M., & Lundberg, E. (2010). A single fixation protocol for proteome-wide immunofluorescence localization studies. *Journal of Proteomics*, *73*, 1067–1078. https://doi.org/10.1016/j.jprot.2009.10.012

Tang, X., Davies, J. E., & Davies, S. J. A. (2003). Changes in distribution, cell associations, and protein expression levels of NG2, neurocan, phosphacan, brevican, versican V2, and tenascin-C during acute to chronic maturation of spinal cord scar tissue. *Journal of Neuroscience Research*, *71*(3), 427–444. https://doi.org/10.1002/jnr.10523

Thumkeo, D., Watanabe, S., & Narumiya, S. (2013). Physiological roles of rho and rho effectors in mammals. *European Journal of Cell Biology*, *92*(10–11), 303–315. https://doi.org/10.1016/j.ejcb.2013.09.002

To, K. C. W., Church, J., & O'Connor, T. P. (2008). Growth cone collapse stimulated by both calpain- and Rho-mediated pathways. *Neuroscience*, *153*(3), 645–653. https://doi.org/10.1016/j.neuroscience.2008.02.043

Vetter, I. R., & Wittinghofer, A. (2001). The guanine nucleotide-binding switch in three dimensions. *Science*, *294*(5545), 1299–1304. https://doi.org/10.1126/science.1062023

Wahl, S., Barth, H., Ciossek, T., Aktories, K., & Mueller, B. K. (2000). Ephrin-A5 Induces Collapse of Growth Cones by Activating Rho and Rho Kinase. *The Journal of Cell Biology*, *149*(2), 263–270. https://doi.org/10.1083/jcb.149.2.263

Wang, H.-X., & Wang, Y.-P. (2016). Gut Microbiota-brain Axis. *Chinese Medical Journal*, *129*(19), 2373–2380. https://doi.org/10.4103/0366-6999.190667

Ward, Y., Yap, S.-F., Ravichandran, V., Matsumura, F., Ito, M., Spinelli, B., & Kelly, K. (2002). The GTP binding proteins Gem and Rad are negative regulators of the Rho-Rho kinase pathway. *The Journal of Cell Biology*, *157*(2), 291–302. https://doi.org/10.1083/jcb.200111026

Wu, K. Y., Hengst, U., Cox, L. J., Macosko, E. Z., Jeromin, A., Urquhart, E. R., & Jaffrey, S. R. (2005). Local translation of RhoA regulates growth cone collapse. *Nature*, *436*(7053), 1020–1024. Retrieved from http://www.nature.com

Ye, X., Qiu, Y., Gao, Y., Wan, D., & Zhu, H. (2019). A Subtle Network Mediating Axon Guidance: Intrinsic Dynamic Structure of Growth Cone, Attractive and Repulsive Molecular Cues, and the Intermediate Role of Signaling Pathways. *Neural Plasticity*, *2019*, 1–26. https://doi.org/10.1155/2019/1719829

Zalar, B., Haslberger, A., & Peterlin, B. (2018). The role of microbiota in depression: a brief review. *Psychiatria Danubina*, *30*(2), 136–141. https://doi.org/10.24869/psyd.2018.136

Zendedel, E., Butler, A. E., Atkin, S. L., & Sahebkar, A. (2018). Impact of curcumin on sirtuins: A review. *Journal of Cellular Biochemistry*, *119*(12), 10291–10300. https://doi.org/10.1002/jcb.27371

ANNEXE

Growth cone assay supplementary material

A

```
> anova<-aov(Área~Muestra, data = experimento)
> summary(anova)
             Df    Sum Sq Mean Sq F value Pr(>F)
Muestra       2   2962404 1481202   0.818  0.443
Residuals   222 402050758 1811039
> tuck <- TukeyHSD(anova)
> (tuck$Muestra <- format(tuck$Muestra, digits = 4, scientific = T, trim = T))
                          diff         lwr          upr         p adj
Fasudil 50uM-Control      "-1.163e+02" "-6.493e+02" "4.168e+02" "8.643e-01"
Fasudil 100uM-Control     "1.515e+02"  "-3.979e+02" "7.009e+02" "7.922e-01"
Fasudil 100uM-Fasudil 50uM "2.678e+02"  "-2.265e+02" "7.620e+02" "4.089e-01"
```

B

```
> anova<-aov(Perímetro~Muestra, data = experimento)
> summary(anova)
             Df  Sum Sq Mean Sq F value Pr(>F)
Muestra       2   62954   31477    1.57   0.21
Residuals   222 4452113   20055
> tuck <- TukeyHSD(anova)
> (tuck$Muestra <- format(tuck$Muestra, digits = 4, scientific = T, trim = T))
                          diff         lwr          upr         p adj
Fasudil 50uM-Control      "3.967e+01"  "-1.643e+01" "9.577e+01" "2.196e-01"
Fasudil 100uM-Control     "3.571e+01"  "-2.210e+01" "9.353e+01" "3.135e-01"
Fasudil 100uM-Fasudil 50uM "-3.956e+00" "-5.596e+01" "4.805e+01" "9.824e-01"
```

Figure Supplementary 1: Acute treatment ANOVAs and Tukey's test results of areas (A) and perimeters (B). Adjusted p-values are higher than .05, non-significant results.

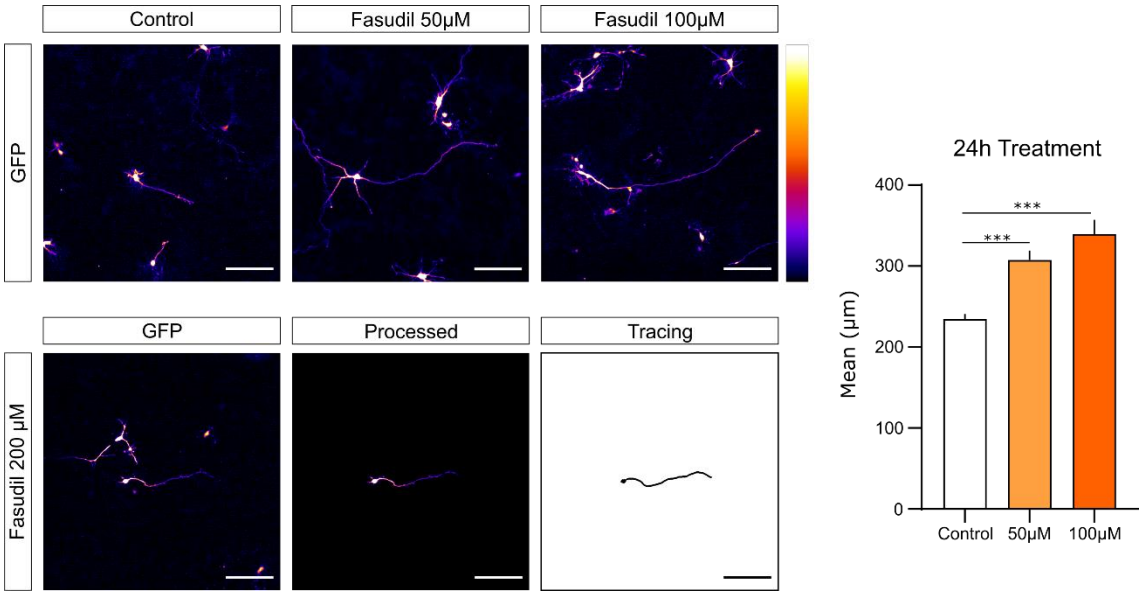

Figure Supplementary 2: 24 hours results: a representative image of each condition. GFP images show non background-removed versions of **Figure 9**. Colour bar represents GFP signal. Also, it is showed raw, processed and tracing of 200 µM. Tracing correspond to the length measured and the drawn soma. Scale bars correspond to 100 µm. Bar plot represents means in µm. Only p-values respect to control are indicated, to see p-value 50 µM – 100 µM see **Figure Suppl. 3**. *** indicates p-value <.001.

```
> anova<-aov(L_norm_micras~Muestra, data = experimento)
> summary(anova)
             Df Sum Sq Mean Sq F value   Pr(>F)
Muestra       3   73.9  24.645    19.2 3.39e-12 ***
Residuals  1344 1724.7   1.283
---
Signif. codes:  0 ‘***’ 0.001 ‘**’ 0.01 ‘*’ 0.05 ‘.’ 0.1 ‘ ’ 1
> tuck <- TukeyHSD(anova)
> (tuck$Muestra <- format(tuck$Muestra, digits = 4, scientific = T, trim = T))
                      diff          lwr          upr          p adj
Fasudil 50-Control      "3.796e-01"  "1.853e-01"  "5.739e-01"  "3.400e-06"
Fasudil 100-Control     "5.788e-01"  "3.635e-01"  "7.941e-01"  "4.261e-11"
Fasudil 200-Control     "1.045e-01"  "-1.884e-01" "3.974e-01"  "7.954e-01"
Fasudil 100-Fasudil 50  "1.992e-01"  "-3.834e-02" "4.368e-01"  "1.359e-01"
Fasudil 200-Fasudil 50  "-2.751e-01" "-5.847e-01" "3.455e-02"  "1.020e-01"
Fasudil 200-Fasudil 100 "-4.743e-01" "-7.976e-01" "-1.511e-01" "9.605e-04"
>
```

Figure Supplementary 3: 24 hours ANOVAs and Tukey’s test results. Adjusted p-values are lower than .001 in pairs with control except Fasudil 200 µM – Control.

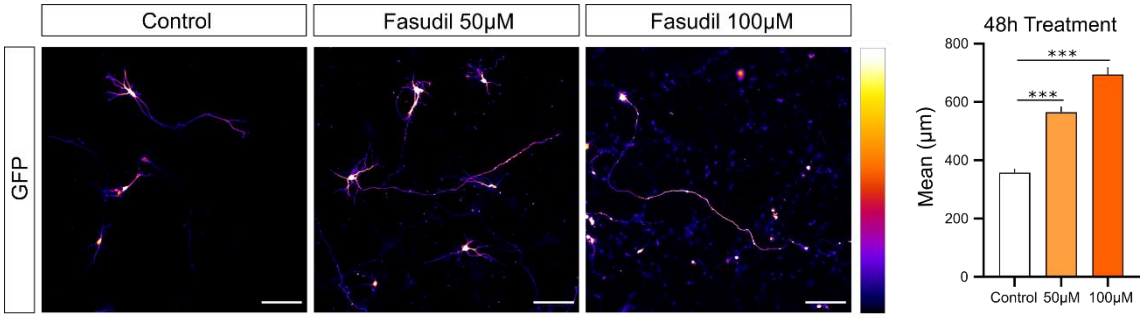

Figure Supplementary 4: 48 hours results: a representative image of each condition. GFP images show non background-removed versions of **Figure 10**. Colour bar represents GFP signal. Also, it is showed raw, processed and tracing of 200 µM. Tracing correspond to the length measured and the drawn soma. Scale bars correspond to 100 µm. Bar plot represents means in µm. Only p-values respect to control are indicated, to see p-value 50 µM – 100 µM see **Figure Suppl. 3**. *** indicates p-value <.001.

```
> anova<-aov(L_norm_micras~Muestra, data = D3D5_total)
> summary(anova)
             Df Sum Sq Mean Sq F value Pr(>F)
Muestra       2   98.8   49.40   72.32 <2e-16 ***
Residuals   829  566.3    0.68
---
Signif. codes:  0 '***' 0.001 '**' 0.01 '*' 0.05 '.' 0.1 ' ' 1
> tuck <- TukeyHSD(anova)
> (tuck$Muestra <- format(tuck$Muestra, digits = 4, scientific = T, trim = T))
                      diff        lwr         upr         p adj
Fasudil 50-Control     "5.799e-01" "4.325e-01" "7.273e-01" "1.790e-13"
Fasudil 100-Control    "8.655e-01" "6.682e-01" "1.063e+00" "1.787e-13"
Fasudil 100-Fasudil 50 "2.856e-01" "8.154e-02" "4.897e-01" "3.037e-03"
```

Figure Supplementary 5: 48 hours ANOVAs and Tukey's test results. Adjusted p-values are lower than .001 in pairs with control.

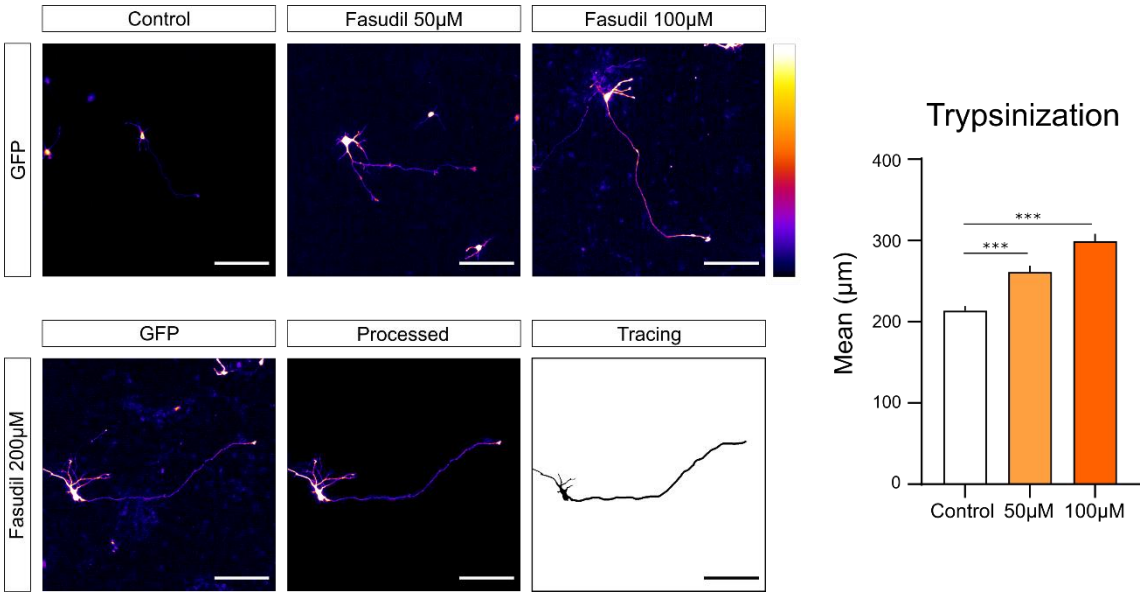

Figure Supplementary 6: Axonal injury and regeneration model results: a representative image of each condition. GFP images show non background-removed versions of **Figure 11**. Colour bar represents GFP signal. Also, it is showed raw, processed and tracing of 200 µM. Tracing correspond to the length measured and the drawn soma. Scale bars correspond to 100 µm. Bar plot represents means in µm. Only p-values respect to control are indicated, to see p-value 50 µM – 100 µM see **Figure Suppl. 7**. *** indicates p-value <.001.

```
> anova<-aov(L_norm~Muestra, data = experimento)
> summary(anova)
             Df Sum Sq Mean Sq F value   Pr(>F)
Muestra       3  20.06   6.687    24.3 5.44e-15 ***
Residuals   724 199.23   0.275
---
Signif. codes:  0 ‘***’ 0.001 ‘**’ 0.01 ‘*’ 0.05 ‘.’ 0.1 ‘ ’ 1
> tuck <- TukeyHSD(anova)
> (tuck$Muestra <- format(tuck$Muestra, digits = 4, scientific = T, trim = T))
                          diff         lwr          upr         p adj
Fasudil 50-Control       "2.253e-01"  "9.975e-02"  "3.509e-01" "2.680e-05"
Fasudil 100-Control      "4.046e-01"  "2.755e-01"  "5.337e-01" "0.000e+00"
Fasudil 200-Control      "3.069e-01"  "1.181e-01"  "4.957e-01" "1.866e-04"
Fasudil 100-Fasudil 50   "1.793e-01"  "3.451e-02"  "3.240e-01" "8.098e-03"
Fasudil 200-Fasudil 50   "8.164e-02"  "-1.182e-01" "2.815e-01" "7.189e-01"
Fasudil 200-Fasudil 100 "-9.763e-02" "-2.997e-01" "1.045e-01" "5.990e-01"
```

Figure Supplementary 3: Axonal injury and regeneration model ANOVAs and Tukey’s test results. Adjusted p-values are lower than .001 in pairs with control.